VILNIUS UNIVERSITY
FACULTY OF CHEMISTRY AND GEOSCIENCES
INSTITUTE OF GEOSCIENCES
DEPARTMENT OF GEOLOGY AND MINERALOGY

Ugnė Birmanaitė
Geology
Master thesis

Relationship between metamorphism and tectonic settings in the Precambrian rocks of Western Lithuania

Scientific adviser
Assoc. prof. Gražina Skridlaitė

Vilnius 2025

VILNIAUS UNIVERSITETAS
CHEMIJOS IR GEOMOKSLŲ FAKULTETAS
GEOMOKSLŲ INSTITUTAS
GEOLOGIJOS IR MINERALOGIJOS KATEDRA

Ugnė Birmanaitė
Geologija
Magistro baigiamasis darbas

Metamorfizmo tipo ryšys su tektonine aplinka prekambro uolienose vakarų Lietuvoje

Darbo vadovė
doc. dr. Gražina Skridlaitė

Vilnius 2025

CONTENTS

INTRODUCTION

The western region of the Precambrian crust in Lithuania is characterized by a complex geology. The underlying crystalline basement, affiliated with the Fennoscandian Shield of the Eastern European Craton, is overlain by a succession of sedimentary rocks (reaching more than 2 km in western Lithuania). The Western Lithuanian granulite domain (WLG) is dominated by felsic and intermediate metaigneous and metasedimentary rocks. Granulites are widespread in the WLG and occupy a large part of the Pociai Basin (Bogdonova et al., 2015). The MLD consists of magmatic rocks, sedimentary rocks occur locally. The WLG has experienced four high-grade metamorphic events during Proterozoic at 1.81-1.79 Ga, 1.73-1.68 Ga, 1.62-1.58 Ga, and 1.52-1.50 Ga (Skridlaite et al., 2014). In previous works, P-T parameters in nearby boreholes were calculated using "GEOTHERMOBAROMETRY" by Skridlaite et al. (2014). Peak conditions obtained were temperature ca. 850°C and pressure ca. 7.5- 8.5 kbar in the Lauksargiai-2 leucocratic domains, while some leucosome and melanosome parts of the granulites in Lauksargiai-2 and Lauksargiai-5 yielded temperatures of 750-780°C at 6.5-7.5 kbar. The phase equilibria modelling with the "THERMOCALC" program was performed by Putnaite et al. (2020) and Skridlaite et al. (2021) for the Lauksargiai-2, 5, and Pociai-1 drillings.

Even though the peak conditions and P-T evolution were defined for some of the rock varieties, metamorphic styles and conditions for some other complexes remained unstudied or poorly studied yet. Therefore, unstudied or less studied rocks exhibiting different metamorphic assemblages were chosen for this study. This work aims to investigate the metamorphism in Western Lithuania (Lauksargiai-1, Bliudziai-150, and Pociai-3 drillings), to review a new material (rock drillcore and thin sections), to analyse the samples for bulk rock composition with X-ray fluorescence spectrometry (XRF), to identify minerals with SEM-EDS (scanning electron microscopy and energy dispersive X-ray spectroscopy), to (re)constrain peak metamorphism (P-T) parameters using phase equilibria modelling with "Perple_X" software applications, to determine age of the peak conditions, and identify the type of metamorphism.

The research will contribute to implications for regional evolution and tectonic setting, heat distribution, and geothermal gradient in Western Lithuania.

1. GEOLOGICAL SETTING

The crystalline basement of Lithuania belongs to the Fennoscandian Shield of the Eastern European Craton and is covered by a thick layer of sedimentary rocks (ranging in thickness from about 200 m to more than 2 km). The East European Craton contains three proto-cratons: Fennoscandia, Sarmatia, and Volgo-Uralia (Gorbatschev and Bogdanova, 1993). Previous works suggested that the Western Lithuanian granulite and the East Lithuanian domains are juxtaposed after the collision of Sarmatia and Fenoscandia along the Mid-Lithuanian suture zone (MLSZ) (Skridlaite and Motuza, 2001). In the recent articles, interpretation and data have been changed (cf. Bogdanova et al., 2015; Skridlaite et al., 2021). The Lithuanian crystalline basement consists of 4 domains: the Western Lithuanian granulite domain (WLG), the Mid-Lithuanian domain (MLD), the Latvian-East Lithuanian (LEL) belt and Belarus-Podlasie granulite (BPG) belt (Fig. 1).

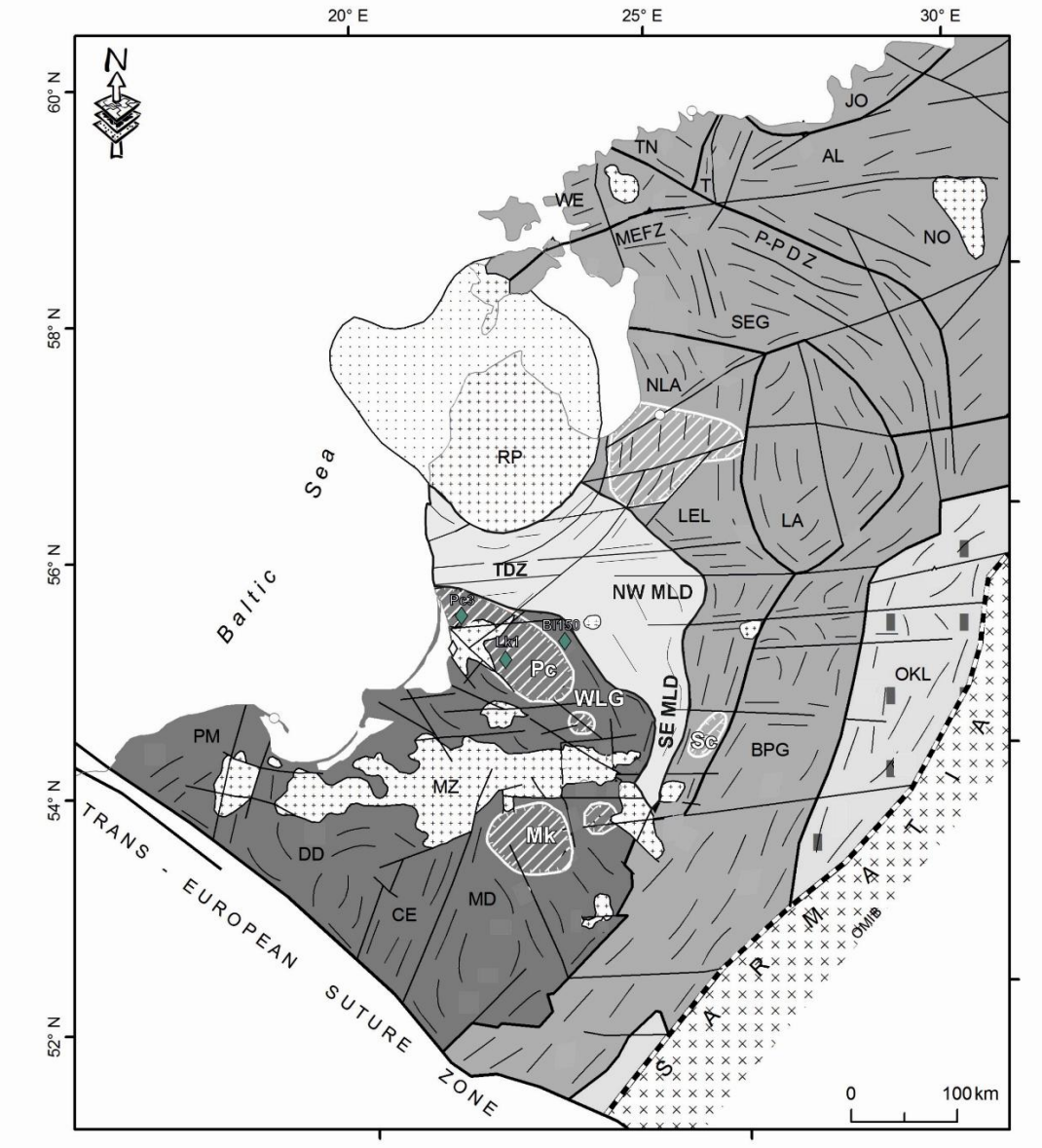

Fig. 1. Crustal structures in the South Baltic region (after Bogdanova et al., 2015). The relevant abbreviations are WLG – Western Lithuania granulite domain, NW (SE) MLD – North Western (South Eastern) Mid-Lithuania domain, LEL – Latvian-East Lithuania domain, and BPG – Belarus-Podlasie granulite domain, Pc – Pociai basin, TDZ – Telsiai deformation zone. The grass green rhombs show Pociai-3 (Pc3), Lauksargiai-1 (Lk1), and Bliudziai-150 (Bl150) boreholes.

The first three domains belong to Fennoscandia, BPG belt may be attributed to Sarmatia (Bogdanova et al., 2016). The WLG domain is composed of felsic and intermediate metaigneous and metasedimentary rocks including charnokitoids and granulites. Granulites are scattered throughout the domain but occupy a large area in the Pociai paleobasin (Bogdanova et al., 2015). The MLD consists of magmatic rocks, whereas sedimentary rocks occur locally. Various charnockites and mafic granulites can be found in the northern and western parts. The MLD magmatic rocks are remnants of continental or oceanic magmatic arcs formed outboard of ca. 1.89 Ga continental margin. In some places, the rocks have been deformed and metamorphosed (Skridlaite et al., 2021). Felsic and mafic metaigneous, also metasedimentary rocks (metagreywackes, marbles) can be found in the Lithuanian part of the LEL belt (Skridlaite and Motuza, 2001). BPG belt is made of large lens-shaped granulite bodies, mylonites and granulites re-equilibrated under amphibolite facies conditions (Bogdonova et al., 1994). The domains differ in rock complexes, structures, lithologies, and metamorphic histories.

Metamorphic rocks in the Precambrian Pociai basin (Fig. 1) are mostly metapelites, but some more silicic varieties of metasediments and minor metaigneous rocks are present. They are crosscut by numerous granitic veins. Some metapelite bodies occur outside the Pociai basin, e.g. the Bliudziai 150 metapelite alternating with metavolcanic pyroxene-bearing gneiss of presumably intermediate composition (andesitic).

2. ANALYTICAL METHODS

Drillcores were inspected at the Underground Information Centre in Vievis, Lithuania. Samples were collected for thin section preparation, analysis of the bulk rock composition, and geochronological dating.

Polished thin sections were prepared from Lauksargiai-1, Pociai-3, and Bliudziai-150 drillcores at the University of Warsaw. All the thin sections were analysed using the Nikon Eclipse 50i POL polarizing microscope, using a magnification of 40-300x. Samples were scanned using the Nikon SZM 1500 polarized microscope with an integrated photosystem, supplied with thin section digital imaging by "Microvisioneer manualWSI" software.

Rock samples were crushed to obtain powder (particle sizes < 5 μm) and powders were sent for a bulk rock composition analysis to the University of Padova (sample from Lauksargiai-1) and Luleå University of Technology (samples from Pociai-3 and Bliudziai-150 drillcores).

From the same samples, the quantitative chemical compositions of garnet, biotite, and plagioclase were obtained by the Quanta 250 SEM (scanning electron microscope). The microstructural study was carried out using BSE (backscatter electron) imaging combined with EDS (Energy-Dispersive Spectrometry) detector X-Max, the INCA x-stream digital pulse processor and the INCA Energy EDS software mineral analysis at the Bedrock geology laboratory of the Nature Research Centre (in Vilnius, Lithuania). An accelerating voltage of 20 kV and 1.0 nA current were used for the analysis. Samples were coated with carbon using Emitech SC7620 Mini Sputter Coater to prevent charging under electron bombardment (Reed, 2005). Analyses were focused on the main mineral phases. The SEM results were recalculated using Microsoft Excel Spreadsheet Software. SEM analyses of garnet, biotite, and feldspars are summarized in Table 4-12. Values of the analyses with a total oxide % between 99 and 101 have been considered for feldspar, 98 and 100 for garnet**,** and for biotite was used values of total dry oxide % sum >95. Most of cordierite and spinel analyses were not accurate (because most of cordierite was affected by pinitization process).

Calculation of P-T equilibrium phase diagrams for a bulk composition has recently been considered the most precise way to thermobarometry in the metamorphic rocks (Powell and Holland, 2010). Thermodynamic modelling of phase equilibria is more complex, considers a larger system, shows relationships between phases and how the composition can differ under different conditions e.g., pressure, temperature (Lanari and Duesterhoeft, 2019). Several software programs exist for calculating phase equilibria, but most used in metamorphic studies are: "THERMOCALC" (Powell and Holland, 1988), "Perple_X" (Connolly, 1990, 2005) and "THERIAK-DOMINO" (de Capitani and Petrakis, 2010). Perple_X is widely used for constraining the crystallization conditions of metamorphic systems, but it has also been applied to granitic systems (e.g. Zhao et al., 2017). Phase equilibrium diagrams (pseudosections) and isopleths for almandine (in chapter 5), Mn in garnet, andesine, and Ti in biotite were calculated using Perple_X 6.9.1 software. Thermodynamic modelling was carried out for all the chosen samples. Applications were used to calculate the P-T pseudosections in the chemical system MnO-Na_2O-CaO-K_2O-FeO-MgO-Al_2O_3-SiO_2-H_2O-TiO_2 (MnNCKFMASHT). There are a few databases used for metapelites, hp62ver (Holland and Powell, 2011) was used in this study. P-T range selected in calculations: 400-1200°C; 2-11 kbar. Pure phases considered in the calculations were quartz, rutile, and Al-silicates. Solid solution models used are melt(W) for melt, Gt(W) for garnet, Opx(W) for orthopyroxene, St(W) for staurolite, Bi(W) for biotite, Mica(W) for mica, Chl(W) for chlorite (White et al., 2001), Sp(HP) for spinel (Holland and Powell, 1996, 1998), Mica(CHA) for mica (Coggon and Holland, 2002; Auzanneu et al., 2010), Ilm(WPH) for ilmenite (White et al., 2000), Pl(h) for plagioclase (Newton et al., 1980), San for K-

feldspar (Waldbaum and Thompson, 1968), hCrd for ideal cordierite and IlGkPy for ideal ilmenite. The final output was re-drawn to obtain results suitable for publication.

Monazite analysis was carried out using the EPMA (electron microprobe analyser) Cameca SX100 at the Institute of Geochemistry, Mineralogy and Petrology, Warsaw University, in Poland. Natural and synthetic materials were used as standards. The analyses were carried out at an accelerating voltage of 20 kV and a beam current of 60 nA, and counting time (peak + background) of 600 s for Pb, 400 s for U, and 200 s for Th. The lines were used in quantitative analysis: Kα lines of P, La, Ca, S and Si; Lα lines of Ce, Er, Yb and Y; Lβ lines of Pr, Nd, Sm, Gd, Tb, Dy and Ho; Mβ lines of Pb and U; Mα line of Th

3. SAMPLE DESCRIPTION

The WLG and MLD rocks vary in appearance, texture, and mineralogy. The Pociai basin (in WLG) was distinguished by Bogdanova et al., (2015). It is comprised of rocks penetrated by Pociai-1-4, Lauksargiai-1,2,5, Silale-3, Taurage-11, and other drillings. These rocks can be described as metasedimentary granulites (Skridlaite and Motuza, 2001**).**

The Lauksargiai-1, Bliudziai-150, Pociai-3 borehole cores were inspected at the Underground Information Centre in Vievis, Lithuania, and the most promising samples were chosen for this study (Table 1).

The sample Lk1D comes from the leucocratic part of the anatectic granulite and contains large garnet grains (up to 4 cm in diameter) surrounded with quartz and feldspar-rich matrix. Sample Pc3/6, on the contrary, was selected from the fine-grained, thin layered, mylonitic gneiss. Bl150 sample represents lens-spotted metapelitic gneiss with leucocratic parts made mostly of cordierite.

Table 1. Characteristics of the studied rocks.

Thin section	Borehole	Depth, m	Coordinates (WGS-84)	Rock name
Lk1D	Lauksargiai-1	1838.2-1839.2	55°09'19.2"N 22°06'60.0"E	Metapelitic gneiss
Bl150	Bliudziai-150	1511	55°15'15.3"N 22°57'53.0"E	Metapelitic gneiss
P3/6	Pociai-3	2154.3	55°30'08.6"N 21°30'05.2"E	Metapelitic mylonite

3.1 Lk1D sample

The thin section obtained from the sample Lk1D contains a porphyroblastic garnet (diameter about 3 cm) rimmed by fine-grained aggregates of biotite, cordierite, symplectites with plagioclase, quartz, and rare K-feldspar grains (Fig. 2a). The porphyroblastic Grt is rounded and has inclusions of quartz, K-feldspar (mostly perthitic) and flakes and segregations of biotite, biotite clots with ore mineral inclusions and monazite. Numerous cracks are filled with cordierite (Fig. 2b). The large garnet is surrounded by leucocratic domains made up from Qtz, K-feldspar, Pl, cordierite, also containing smaller euhedral and skeletal garnet grains (up to 2 mm) surrounded mostly with cordierite and spinel intergrowths (Fig. 2a). Some of the small garnet grains are overgrown by thin biotite aggregates with minor cordierite, and K-feldspar. There are also elongated domains of cordierite with biotite, sillimanite, spinel, and ore mineral inclusions. The rock also features thin strips of sillimanite with spinel and ore minerals.

Ore minerals are mostly ilmenite, rutile, and spinel. Other accessory minerals are apatite and monazite.

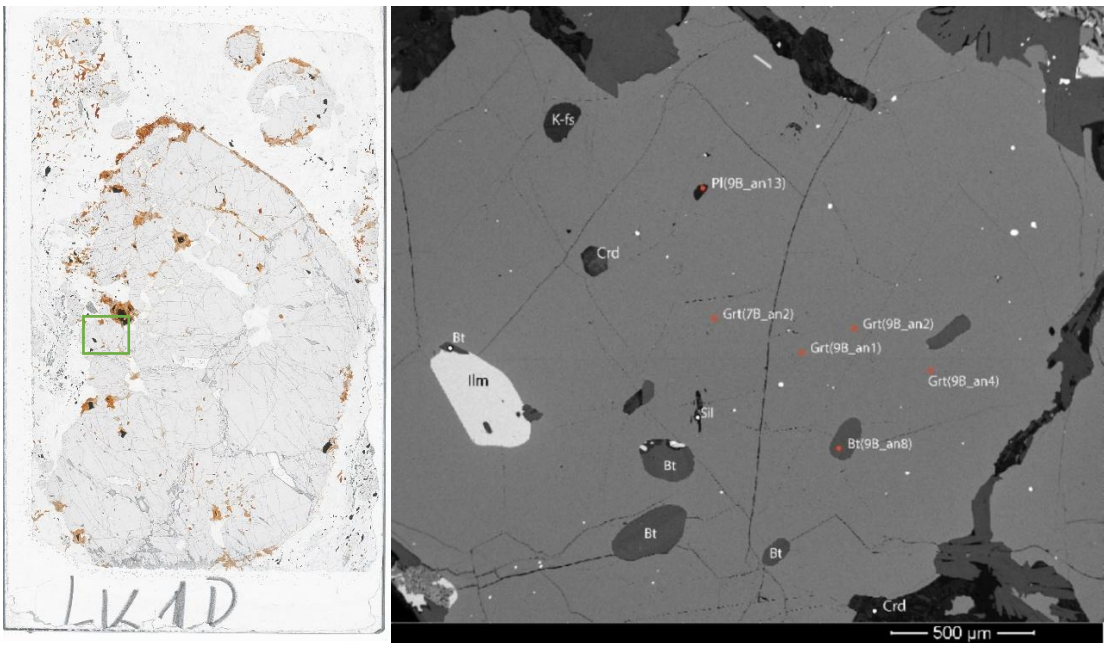

Fig. 2. Scanned image of the sample Lk1D (a) and SEM-BSE-image of the granulite (b). Green square shows location of the SEM-BSE image (a). Red dots mark places of SEM-EDS analysis (b). Abbreviations: Bt – biotite, Crd – cordierite, Grt – garnet, Ilm – ilmenite, K-fs – potassium feldspar, Pl – plagioclase, Sil – sillimanite.

3.2 Bl150 sample

The thin section obtained from sample Bliudziai-150 exhibits a lens-spotted texture, characterised by leucocratic granitic domains and lens-shaped aggregates of dark minerals (Fig. 3). Melanocratic domains are composed of spinel (Spl) – cordierite (Crd) symplectites surrounding sillimanite (Sil) and opaque cores. Garnet (Grt) occurs as irregularly shaped grains, as well as smaller euhedral and skeletal garnet grains (up to 2 mm) surrounded mostly with K-feldspar, cordierite and spinel intergrowths. Biotite (Bt) hosts inclusions of monazite (Mnz). Melanocratic lenses are surrounded by irregularly shaped domains of quartz (Qtz), Crd and K-feldspar (Kfs).

Ore minerals are mostly spinel, ilmenite, and rutile. Zircon, monazite and apatite grains are also abundant.

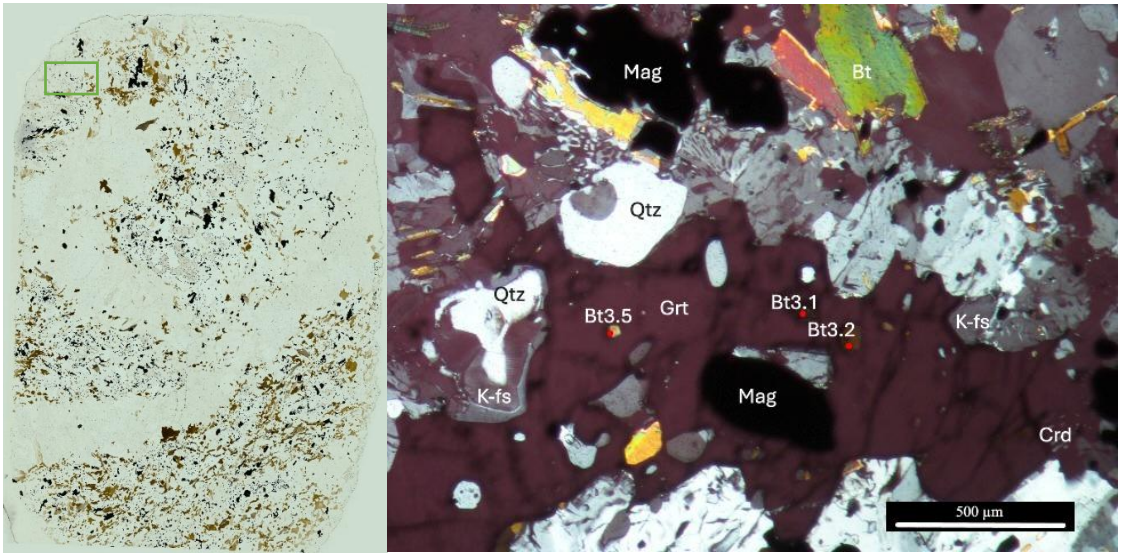

Fig. 3. Scanned image of the sample BL150 (a) and XPL image of the metapelite (b). Green square shows location of the XPL image (a). Abbreviations: Bt – biotite, Crd – cordierite, Grt – garnet, K-fs – K-feldspar, Mag – magnetite, Qtz – quartz.

3.3 Pc3/6 sample

The thin section from sample P3/6 reveals a layered structure composed of several mineral assemblages (Fig. 4a). The main rock-forming minerals include garnet (Grt), quartz (Qtz), K-feldspar (Kfs), and cordierite (Crd), with biotite (Bt), and minor plagioclase (Pl) also present. Garnet occurs as both coarse porphyroblasts and finer grains. Garnet grains contain inclusions of cordierite, quartz, biotite, and ore minerals (Fig. 4b). A fine-grained mylonitic foliation is defined by ribbon quartz, with all minerals generally aligned along a common foliation plane (Fig. 4a).

The ore minerals are mostly ilmenite, magnetite, rutile, and spinel. Other accessory minerals observed include monazite, zircon, pyrite, chalcopyrite. Biotite is often replaced by chlorite, while ilmenite decays into rutile and magnetite.

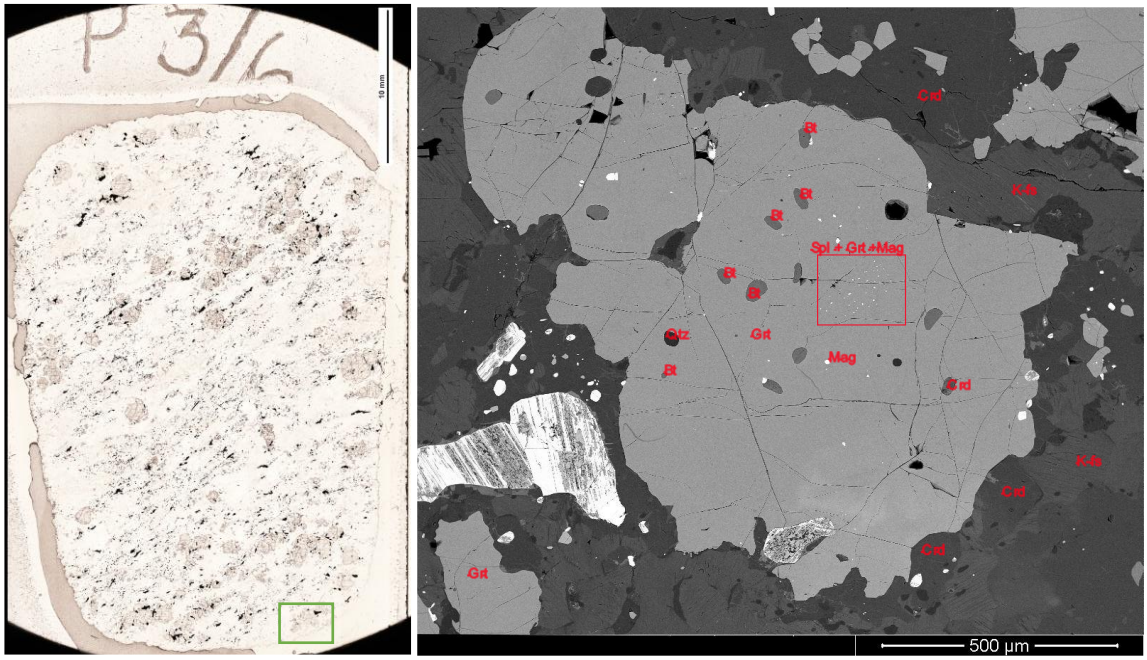

Fig. 4. Scanned image of the sample Pc3/6 (a) and SEM-BSE-image of the mylonite (b). Green square shows location of the SEM-BSE-image (b). Abbreviations: Bt – biotite, Crd – cordierite, Grt – garnet, K-fs – K-feldspar, Mag – magnetite, Qtz – quartz, Spl – spinel. Red square shows spinel and magnetite in garnet core.

4. ROCK AND MINERAL CHEMISTRY

The bulk composition of the selected samples is provided as weight percent of oxides (wt%) in **Table 2**. Even though there are no big differences in SiO_2 and Al_2O_3 contents the FeO, MgO, CaO, Na_2O, and K_2O contents are variable.

The sample Lk1D consists mainly of porphyroblastic garnet (Fig. 2), minor biotite and K-feldspar, therefore it has the highest throughout Fe_2O_3 (15.39 wt%) and the lowest K_2O (1.51 wt%) contents. It is rich in ilmenite, which is reflected in the high content of TiO_2 of1.31 wt%. Ca-rich plagioclase can account for the high CaO (1.81 wt%). The sample Bl150 has the lowest Fe_2O_3 (11.20 wt%) and MgO (3.90 wt%) but higher Al_2O_3 (26.92 wt%) and Na_2O (2.04 wt%). The sample Pc3/6 lacks plagioclase in the mineral assemblage, which is reflected in the low content of CaO (0.36 wt.%). Also, Pc3/6 has the highest amount of MgO (4.58 wt%).

Table 2. Major element bulk composition (wt.%) of the selected samples.

	Lk1D	**BL150**	**Pc3/6**
SiO_2	48.32	48.01	51.30
TiO_2	1.31	1.08	1.60
Al_2O_3	25.86	26.92	24.50
Fe_2O_3 tot.	15.39	11.20	12.70
MnO	0.18	0.18	0.09
MgO	4.04	3.90	4.58
CaO	1.81	1.30	0.23
Na_2O	1.89	2.04	1.07
K_2O	1.51	4.32	4.35
P_2O_5	0.05	0.18	0.22
Total	100.36	99.13	100.64
FeO tot.	13.85	10.08	11.43

For the phase equilibria modelling, the mineral chemistry of the samples must be taken into account.

4.1 Garnet

*The sample **Lk1D*** contains two types of garnets. The porphyroblastic garnet is generally rich in almandine and pyrope solid solutions, but poor in grossular and spessartine (Table 3). Almandine values can vary from 70.8 to 72.5 in the core and from 72.3 to 84.1 in the rim. Pyrope values can differ from 23.2 to 24.7 in the core and from 10.6 to 23.5 in the rim. Grossular values are from 2.4 to 3.1 in the core and from 2.4 to 3.7 in the rim. Spessartine values can reach from 1.2 to 2.0 in the core and from 1.2 to 2.1 in the rim (Table 3). Garnets are quite homogeneous from core to rim, but there are some composition changes in places (e.g. Mg and Fe amounts near contact with biotite).

Smaller garnets (sample Lk1D) have a bit different composition. They are considerably richer in almandine (min 81.4, max 83.5), and poorer in pyrope (min 11.7, max 14.0), with grossular (min 2.7, max 3.1), and spessartine (min 1.6, max 2.0) (Table 3).

Table 3. Representative SEM-EDS mineral analyses of garnet from the sample Lk1D.

Sample (wt%)	**Lk1D**							
Analysis number	6A_an4	6A_an7	7A_an1	7B_an2	9B_an1	9B_an2	9B_an4	1C_an2
	Grt core	Grt core	Grt rim	Grt rim	Grt rim	Grt rim	Grt rim	Smaller grt
SiO_2	38.09	38.24	37.63	37.59	37.67	37.90	37.89	36.44
TiO_2	0.00	0.00	0.00	0.00	0.00	0.00	0.00	0.00
Al_2O_3	21.44	21.30	21.10	21.28	21.35	21.66	21.46	20.89
FeO	32.61	32.82	33.37	32.65	32.57	33.35	32.92	36.68
Fe_2O_3 (calc)	0.21	0.67	1.01	1.33	0.79	0.71	0.60	0.32
MgO	6.24	6.16	5.50	5.84	5.86	5.68	5.85	2.85
MnO	0.71	0.61	0.60	0.73	0.74	0.72	0.61	0.87
CaO	0.85	1.02	0.95	0.90	1.00	0.87	1.05	0.96
Sum (dry)	100.15	100.82	100.16	100.31	99.98	100.89	100.38	98.71
Number of ions based on 12 anions								
Si	3.00	3.00	2.98	2.97	2.98	2.98	2.99	2.98
Ti	0.00	0.00	0.00	0.00	0.00	0.00	0.00	0.00
Al	1.99	1.97	1.97	1.98	1.99	2.00	1.99	2.02
Fe^{2+}	2.15	2.15	2.21	2.16	2.16	2.19	2.17	2.49
Fe^{3+}	0.01	0.04	0.06	0.08	0.05	0.04	0.04	0.02
Mg	0.73	0.72	0.65	0.69	0.69	0.67	0.69	0.35
Mn	0.05	0.04	0.04	0.05	0.05	0.05	0.04	0.06
Ca	0.07	0.09	0.08	0.08	0.08	0.07	0.09	0.08
Sum (Cat)	8.00	8.00	8.00	8.00	8.00	8.00	8.00	8.00
% end members								
Almandine	71.6	71.8	74.2	72.6	72.3	73.6	72.7	83.5
Pyrope	24.4	24.0	21.8	23.2	23.2	22.3	23.0	11.7
Spessartine	1.6	1.4	1.4	1.6	1.7	1.6	1.4	2.0
Grossular	2.4	2.8	2.6	2.5	2.8	2.4	2.9	2.8
Mg/(Fe+Mg)	0.254	0.251	0.227	0.242	0.243	0.233	0.241	0.123

The sample ***BL150*** contains the garnets, that are mostly almandine, spessartine, and pyrope solid solutions with small grossular component. They have much higher spessartine values (from 14.42 to 18.36) than the other garnets (Tables 3, 4 and 5). Almandine values can vary from 63.83 to 67.04. Pyrope values can differ from 13.16 to 18.08. Grossular values are from 2.33 to 2.77 (Table 4).

Table 4. Representative SEM-EDS mineral analyses of garnet from the sample BL150.

Sample (wt%)	**BL150**							
Analysis number	Bl150grt 1.22r	Bl150grt1. 23r	Bl150grt 1.7c	Bl150grt 1.18c	Bl150grt 4.29c	Bl150grt 4.30c	Bl150grt 4.24	Bl150grt4. 26r
SiO_2	36.74	36.85	36.76	36.67	36.68	36.92	36.94	36.80
TiO_2	0.08	0.06	0.06	0.06	0.01	0.00	0.00	0.05
Al_2O_3	21.11	21.30	21.37	21.27	21.21	21.25	21.23	21.19
FeO	28.29	28.43	28.57	28.61	28.11	28.52	28.73	28.42
Fe_2O_3 (calc)	1.67	1.36	0.99	1.24	1.27	1.06	0.51	0.78
MgO	3.91	3.93	3.68	3.60	3.92	3.86	3.56	3.85
MnO	7.57	7.50	7.53	7.52	7.57	7.43	7.85	7.55
CaO	0.84	0.85	0.98	0.98	0.86	0.95	0.89	0.87
Sum (dry)	100.21	100.28	100.00	99.95	99.64	100,.05	99.71	99.52
Number of ions based on 12 anions								
Si	2.947	2.950	2.953	2.950	2.954	2.962	2.977	2.967
Ti	0.005	0.004	0.004	0.004	0.001	0.000	0.000	0.003
Al	1.996	2.010	2.023	2.017	2.013	2.009	2.016	2.013
Fe^{2+}	1.898	1.903	1.919	1.925	1.893	1.914	1.936	1.916
Fe^{3+}	0.101	0.082	0.060	0.075	0.077	0.064	0.031	0.048
Mg	0.468	0.469	0.441	0.432	0.471	0.462	0.428	0.463
Mn	0.514	0.509	0.512	0.512	0.516	0.505	0.536	0.516
Ca	0.072	0.073	0.084	0.084	0.074	0.082	0.077	0.075
Sum (Cat)	8.000	8.000	8.000	8.000	8.000	8.000	8.000	8.000
% end members								
Almandine	64.3	64.4	64.9	65.2	64.1	64.6	65.1	64.5
Pyrope	15.8	15.9	14.9	14.6	15.9	15.6	14.4	15.6
Spessartine	17.4	17.2	17.3	17.3	17.5	17.0	18.0	17.4
Grossular	2.3	2.4	2.8	2.8	2.4	2.7	2.5	2.5
Mg/(Fe+Mg)	0.198	0.198	0.187	0.183	0.199	0.194	0.181	0.194

The sample ***Pc3/6*** contains one type of garnet. They are quite homogeneous from core to rim (Fig. 5), but there are some compositional changes in places (e.g. Mg-Fe near contact with cordierite).

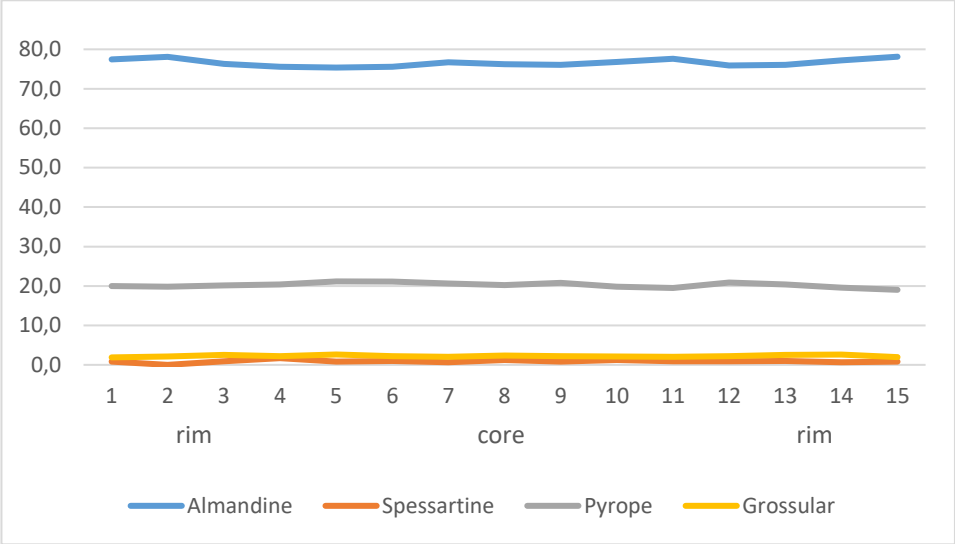

Fig. 5. Compositional rim-core-rim profile across representative garnet crystal in the sample Pc3/6.

The garnets are generally rich in almandine and pyrope, but poor in grossular and spessartine (Table 5). Almandine values can vary from 73.17 to 78.31. Pyrope values can differ from 18.78 to 23.41. Grossular values are from 1.49 to 2.63. Spessartine values can reach from 0 to 1.70 (Table 5).

Table 5. Representative SEM-EDS mineral analyses of garnet from the sample Pc3/6.

Sample (wt%)	**Pc3/6**									
Analysis number	2.2	2.9	2.17	3.2	3.9	3.14	16.7	16.12	18.18	18.19
	Grt rim	Grt core	Grt rim	Grt rim	Grt core	Grt rim	Grt rim	Grt core	Grt core	Grt core
SiO_2	37.61	37.70	36.91	37.63	37.59	37.92	37.29	37.63	38.36	38
TiO_2	0.00	0.00	0.00	0.00	0.00	0.00	0.00	0.00	0.00	0.00
Al_2O_3	20.80	20.96	21.02	20,99	20.74	20.46	20.96	21.31	21.2	21.18
FeO	34.43	34.56	34.48	33.80	33.51	33.85	34.27	34.39	34.27	33.54
Fe_2O_3 (calc)	0.00	0.11	0.74	0.93	0.42	0.32	0.94	0.00	0.00	0.00
MgO	4.99	5.21	4.71	5.43	5.73	5.83	4.90	5.21	5.43	5.79
MnO	0.55	0.29	0.37	0.57	0.34	0.00	0.46	0.44	0.47	0.38
CaO	0.77	0.73	0.69	0.73	0.69	0.86	0.87	0.52	0.77	0.56
Sum (dry)	99.15	99.56	98.92	100.08	99.01	99.24	99.69	99.50	100.50	99.45
Si	3.019	3.010	2.978	2.990	3.009	3.028	2.984	3.003	3.025	3.019
Ti	0.000	0.000	0.000	0.000	0.000	0.000	0.000	0.000	0.000	0.000
Al	1.968	1.973	1.999	1.965	1.957	1.925	1.976	2.004	1.970	1.983

Fe^{2+}	2.311	2.308	2.327	2.246	2.243	2.260	2.293	2.295	2.260	2.228
Fe^{3+}	0.000	0.006	0.045	0.056	0.025	0.019	0.057	0.000	0.000	0.000
Mg	0.597	0.620	0.567	0.643	0.684	0.694	0.584	0.620	0.638	0.686
Mn	0.037	0.020	0.025	0.038	0.023	0.000	0.031	0.030	0.031	0.026
Ca	0.066	0.062	0.060	0.062	0.059	0.074	0.075	0.044	0.065	0.048
Sum (Cat)	7.998	8.000	8.000	8.000	8.000	8.000	8.000	7.995	7.990	7.989
Almandine	76.8	76.7	78.1	75.1	74.5	74.7	76.9	76.9	75.7	74.9
Pyrope	19.8	20.6	19.0	21.5	22.7	22.9	19.6	20.6	21.1	22.7
Spessartine	1.2	0.7	0.8	1.3	0.8	0.0	1.0	1.0	1.0	0.8
Grossular	2.2	2.1	2.0	2.0	1.9	2.4	2.4	1.5	2.2	1.6
Mg/(Fe+Mg)	0.205	0.212	0.196	0.223	0.234	0.235	0.203	0.213	0.220	0.235

4.2 Biotite

*The sample **Lk1D.*** Biotite shows a large variation in chemical composition (Table 6). The average Ti content in biotite is 0.425 (apfu). The average X_{Mg} (Mg/(Mg+Fe)) is 0.634. The highest titanium content (0.716 apfu) has been found in biotite (analysis 9B_an8), which is present as an inclusion in the garnet (Fig. 2b). FeO and MgO contents vary in ranges of 10.4 – 16.3 wt% and 12.98 – 18.31wt% respectively, having the highest MgO in rims adjacent to the garnet.

Table 6. Representative SEM-EDS mineral analyses of biotite from the sample Lk1D.

Sample (wt%)	**Lk1D**							
Analysis number	9A_an4	9B_an8	10B_an5	10B_an6	10B_an8	11B_an9	11B_an10	12B_an5
SiO_2	36.57	36.63	37.06	37.01	38.55	38.05	39.05	37.32
TiO_2	3.74	6.46	5.62	4.99	2.44	2.83	0.82	4.23
Al_2O_3	16.01	16.59	16.64	16.34	16.46	16.18	16.88	15.94
FeO	16.3	13.15	13.38	13.45	10.40	12.44	10.84	15.27
MgO	12.98	13.05	13.58	14.41	18.04	15.57	18.31	13.32
MnO	0.00	0.00	0.00	0.16	0.00	0.00	0.00	0.00
CaO	0.00	0.00	0.00	0.00	0.00	0.00	0.00	0.00
Na_2O	0.00	0.34	0.28	0.25	0.00	0.00	0.00	0.00
K_2O	9.63	9.67	9.65	9.69	9.82	10.01	9.65	9.83
F	1.17	0.62	0.74	0.83	2.29	1.61	2.19	1.19
H_2O (calc.)	3.43	3.77	3.73	3.69	3.05	3.30	3.10	3.47
Sum	99.34	100.02	100.37	100.47	100.09	99.31	99.91	100.07
Si	5.50	5.40	5.44	5.44	5.590	5.62	5.66	5.55
Al^{IV}	2.50	2.60	2.56	2.56	2.410	2.38	2.34	2.46

Al^{VI}	0.34	0.28	0.32	0.27	0.403	0.44	0.55	0.34
Ti	0.42	0.72	0.62	0.55	0.266	0.31	0.09	0.47
Fe^{2+}	2.05	1.62	1.64	1.65	1.261	1.54	1.32	1.90
Mg	2.91	2.87	2.97	3.16	3.899	3.43	3.96	2.95
Mn	0.00	0.00	0.00	0.02	0.000	0.00	0.00	0.00
Ca	0.00	0.00	0.00	0.00	0.000	0.00	0.00	0.00
Na	0.00	0.10	0.08	0.07	0.000	0.00	0.00	0.00
K	1.85	1.82	1.81	1.82	1.816	1.89	1.79	1.86
X_{Mg}	0.587	0.639	0.64	0.66	0.756	0.690	0.751	0.609

*The sample **Bl150***. The average Ti content in biotite is 0.433 (apfu). The average X_{Mg} is 0.620. The highest titanium content (0.641) has been found in central part (core) of the biotite (Table 7; analysis Bl150bt5.17c), which is present near contact with garnet. It also contains the highest MnO (up to 0.25 wt%).

Table 7. Representative SEM-EDS mineral analyses of biotite from the sample Bl150.

Sample (wt%)	**BL150**							
Analysis number	Bl150/ 14	Bl150bt 1.1r	Bl150bt 3.1	Bl150bt 3.2	Bl150bt4. 1inc	Bl150bt4. 2inr	Bl150bt5. 8or	Bl150bt5 .17c
SiO_2	36.56	36.21	35.80	35.74	36.17	35.67	36.00	35.80
TiO_2	2.13	3.87	3.19	3.13	4.34	4.92	4.10	5.74
Al_2O_3	19.45	17.44	19.44	19.41	17.49	16.96	17.67	16.91
FeO	12.83	15.42	16.48	16.10	14.86	14.40	14.51	14.89
MnO	0.10	0.07	0.19	0.19	0.17	0.11	0.17	0.25
MgO	15.31	13.67	10.77	10.65	13.08	12.98	13.16	12.84
CaO	0.00	0,00	0.04	0.02	0.00	0.01	0.03	0.00
Na_2O	0.00	0,00	0.12	0.13	0.16	0.30	0.15	0.00
K_2O	8.56	9.75	9.67	9.74	10.11	9.83	10.06	9.88
Cr_2O_3	0.00	0.00	0.04	0.00	0.06	0.06	0,11	0.00
H_2O (calc.)	4.08	4.05	4.01	3.99	4.05	4.00	4.03	4.04
Sum	99.02	100.48	99.74	99.10	100.50	99.22	99.98	100.35
Si	5.369	5.359	5.353	5.372	5.357	5.345	5.351	5.313
Al^{IV}	2.631	2.641	2.647	2.628	2.643	2.655	2.649	2.687
Al^{VI}	0.736	0.403	0.779	0.811	0.410	0.340	0.447	0.272
Ti	0.235	0.431	0.359	0.353	0.483	0.554	0.458	0.641
Cr	0.000	0.000	0.005	0.000	0.007	0.007	0.012	0.000
Fe^{2+}	1.576	1.909	2.061	2.024	1.841	1.804	1.803	1.848

Mn	0.012	0.009	0.024	0.024	0.021	0.013	0.021	0.031
Mg	3.351	3.017	2.400	2.387	2.889	2.899	2.916	2.840
Ca	0.000	0.000	0.006	0.003	0.000	0.001	0.005	0.000
Na	0.000	0.000	0.035	0.036	0.046	0.086	0.042	0.000
K	1.604	1.841	1.844	1.868	1.910	1.879	1.907	1.870
X_{Mg}	0.680	0.612	0.538	0.541	0.611	0.616	0.618	0.606

In the analysed *sample* ***Pc3/6,*** biotite is predominantly observed as inclusions within garnet. The average Ti content in biotite is 0.584 (apfu). The average X_{Mg} is 0.659. The highest titanium content (0.713 apfu) has been found in the matrix biotite (Table 8; analysis 14.4), which is present in cordierite.

Table 8. Representative SEM-EDS mineral analyses of biotite from the sample Pc3/6.

Sample (wt%)	**Pc3/6**							
Analysis number	3.24	3.25	4.19	9.23	14.4	16.19	19.4	19.9
SiO_2	36.66	37.42	37.22	37.48	36.44	37.41	38.23	37.86
TiO_2	5.35	5.57	5.64	4.99	6.30	5.58	5.27	5.35
Al_2O_3	15.5	15.82	15.76	15.48	15.29	16.00	15.41	15.47
FeO	11.95	12.27	13.42	13.58	18.00	12.72	11.18	12.02
MnO	0.00	0.00	0.00	0.00	0.00	0.00	0.00	0.00
MgO	15.04	15.18	14.16	14.96	10.59	14.19	15.94	15.49
CaO	0.00	0.00	0.00	0.00	0.00	0.00	0.00	0.00
Na_2O	0.44	0.55	0.00	0.00	0.00	0.00	0.00	0.28
K_2O	9.42	9.51	9,44	9.63	9.49	9.88	9.79	9,77
F	1.21	1.01	1.06	1.53	0.00	1.24	1.52	0.97
H_2O (calc.)	3.46	3.63	3.56	3.35	3.99	3.49	3.39	3.65
Sum	99.43	100.96	99.82	100.36	100.10	99.99	100.09	100.86
Si	5.453	5.464	5.490	5.510	5.480	5.502	5.570	5.525
Al^{IV}	2.547	2.536	2.510	2.490	2.520	2.498	2.430	2.475
Al^{VI}	0.17	0.186	0.231	0.193	0.191	0.275	0.217	0.185
Ti	0.598	0.612	0.626	0.552	0.713	0.617	0.577	0.587
Fe^{2+}	1.486	1.498	1.656	1.670	2.264	1.564	1.362	1.467
Mn	0.000	0.000	0.000	0.000	0.000	0.000	0.000	0.000
Mg	3.335	3.304	3.114	3.279	2.374	3.111	3.462	3.369
Ca	0.000	0.000	0.000	0.000	0.000	0.000	0.000	0.000
Na	0.127	0.156	0.000	0.000	0.000	0.000	0.000	0.079

K	1.787	1.771	1.776	1.806	1.820	1.853	1.820	1.818
X_{Mg}	0.692	0.688	0.653	0.663	0.512	0.665	0.718	0.697

4.3 Feldspars

Distribution and amounts of feldspars vary greatly from sample to sample. The sample ***Lk1D*** contains feldspars, which occur in leucocratic domains, also as an inclusions in garnet. Plagioclases are without zoning, mostly andesine with An (anorthite) content ranging from 30 to 37 wt% (Table 9). The content of K_2O varies from 0.00 to 0.24 wt% in plagioclases, from 12.49 to 13.20 wt% in K-feldspars.

Table 9. Representative SEM-EDS mineral analyses of feldspars from the sample Lk1D.

Sample (wt%)	**Lk1D**							
Analysis number	11A_an5	11A_an3	12A_an5	13A_an1	13A_an2	13A_an6	13A_an7	9B_an13
SiO_2	60.19	58.29	60.05	59.15	59.23	58.74	58.66	59.17
TiO_2	0.00	0.00	0.00	0.00	0.00	0.00	0.00	0.00
Al_2O_3	24.82	25.59	25.49	24.92	25.03	25.60	26.08	25.36
FeO	0.00	0.20	0.00	0.21	0.00	0.00	0.00	0.51
MnO	0.17	0.00	0.00	0.00	0.00	0.00	0.00	0.00
CaO	6.57	7.42	6.97	6.48	6.96	7.98	8.16	7.57
Na_2O	8.20	7.67	7.94	8.09	7.84	7.61	7.52	7.59
K_2O	0.12	0.10	0.00	0.24	0.20	0.17	0.00	0.13
Sum	100.08	99.27	100.45	99.09	99.26	100.10	100.57	100.33
Number of ions based on 8 O								
Si	2.68	2.63	2.66	2.67	2.66	2.63	2.61	2.64
Ti	0.00	0.00	0.00	0.00	0.00	0.00	0.00	0.00
Al	1.30	1.36	1.33	1.32	1.33	1.35	1.37	1.34
Fe^{2+}	0.00	0.01	0.00	0.01	0.00	0.00	0.00	0.02
Mn	0.01	0.00	0.00	0.00	0.00	0.00	0.00	0.00
Ca	0.31	0.36	0.33	0.31	0.34	0.38	0.39	0.36
Na	0.71	0.67	0.68	0.71	0.68	0.66	0.65	0.66
K	0.01	0.01	0.00	0.01	0.01	0.01	0.01	0.01
Sum Cations	5.02	5.03	5.01	5.03	5.02	5.03	5.03	5.02
% end members								
$NaAlSi_3O_8$ (Ab)	68.852	64.802	67.336	68.393	66.341	62.729	62.006	64.004

$CaAl_2Si_2O_8$ (An)	30.485	34.642	32.664	30.273	32.545	36.349	37.181	35.275
$KAlSi_3O_8$ (Kfs)	0.663	0.556	0.000	1.335	1.113	0.922	0.814	0.721

The sample ***Bl150*** contains feldspars, which occur in leucocratic domains. Plagioclases are without zoning, mostly oligoclase and andesine with An (anorthite) content ranging from 27 to 33 wt% (Table 10). The content of K_2O varies from 0.042 to 0.128 wt% in plagioclases.

Table 10. Representative SEM-EDS mineral analyses of feldspars from the sample Bl150.

Sample (wt%)	**Bl150**							
Analysis number	Bl150pl1.4c	Bl150pl1.2c	Bl150pl1.1c	Bl150pl1.5r	Bl150pl4.11	Bl150pl4.12	Bl150pl4.13	Bl150pl4.15
SiO_2	59.9	61.002	61.003	60.875	59.394	59.951	60.411	59.929
Al_2O_3	25.377	25.233	25.308	24.899	25.615	25.951	25.27	25.953
FeO	0.009	0.076	0.136	0.097	0.15	0.179	0.164	0.143
CaO	6.112	5.691	5.699	5.438	6.717	6.685	6.127	6.738
Na_2O	7.76	8.026	8.048	8.16	7.504	7.316	7.944	7.645
K_2O	0.11	0.099	0.094	0.042	0.066	0.128	0.095	0.076
Sum	99.268	100.127	100.288	99.511	99.446	100.21	100.011	100.484
Number of ions based on 8 O								
Si	2.680	2.702	2.699	2.711	2.659	2.660	2.685	2.655
Al	1.338	1.317	1.320	1.307	1.352	1.357	1.324	1.355
Fe^{2+}	0.000	0.003	0.005	0.004	0.006	0.007	0.006	0.005
Ca	0.293	0.270	0.270	0.260	0.322	0.318	0.292	0.320
Na	0.673	0.689	0.690	0.705	0.651	0.630	0.685	0.657
K	0.006	0.006	0.005	0.002	0.004	0.007	0.005	0.004
Sum Cations	4.991	4.987	4.989	4.989	4.993	4.979	4.998	4.997
% end members								
$NaAlSi_3O_8$ (Ab)	69.225	71.431	71.480	72.905	66.647	65.943	69.731	66.953
$CaAl_2Si_2O_8$ (An)	30.130	27.989	27.971	26.848	32.967	33.298	29.720	32.609
$KAlSi_3O_8$ (Kfs)	0.646	0.580	0.549	0.247	0.386	0.759	0.549	0.438

Petrographic and SEM-EDS analysis revealed that the sample ***Pc3/6*** is predominated by K-feldspar and has very little plagioclase, occurring in a few spots. Plagioclases differ from those in

the LkD and Bl150 samples by much lower CaO content and are mostly oligoclases with An content ranging from 15 to 22 (Table 11). The content of K_2O varies from 0.00 to 0.24 wt% in plagioclases, from 12.69 to 13.93 wt% in K-feldspars.

Table 11. Representative SEM-EDS mineral analyses of feldspars from the sample Pc3/6.

Sample (wt%)	**Pc3/6**									
Analysis number	2.22	2.29	3.33	11.3	11.5	11.8	16.22	17.8	17.12	17.13
SiO_2	64.66	64.09	65.34	62.61	62.71	62.67	64.32	64.78	63.86	62.90
Al_2O_3	18.44	18.13	18.5	23.11	23.21	23.17	22.76	21.83	22.43	23.65
FeO	0.42	0.5	0.00	0.00	0.00	0.29	0.00	0.00	0.00	0.00
CaO	0.00	0.00	0.00	4.56	4.56	4.61	3.67	3.19	3.62	4.36
Na_2O	3.32	1.72	2.05	9.76	9.34	9.29	9.78	10.18	9.76	9.15
K_2O	12.69	13.93	13.85	0.00	0.00	0.00	0.00	0.00	0.22	0.24
Sum	99.53	99.24	99.74	100.04	99.82	100.03	100.53	99.98	99,89	100,30
Number of ions based on 8 O										
Si	2.980	2.973	3,001	2,776	2,781	2,778	2,823	2,856	2,825	2,775
Al	1.002	1.007	1.001	1.208	1.213	1.210	1.177	1.134	1.169	1.230
Fe^{2+}	0.016	0.019	0.000	0.000	0.000	0.011	0.000	0.000	0.000	0.000
Ca	0.00	0.000	0.000	0.217	0.217	0.219	0.173	0.151	0.172	0.206
Na	0.297	0.154	0.183	0.839	0.803	0.798	0.832	0.870	0.837	0.783
K	0.746	0.822	0.811	0.000	0.000	0.000	0.000	0.000	0.012	0.014
Sum Cations	5.041	4.990	4.996	5.040	5.014	5.016	5.005	5.012	5.015	5.008
% end members										
$NaAlSi_3O_8$ (Ab)	28.454	15.804	18.368	79.480	78.753	78.479	82.825	85.240	81.981	78.090
$CaAl_2Si_2O_8$ (An)	0.000	0.000	0.000	20.520	21.247	21.521	17.175	14.760	16.803	20.562
$KAlSi_3O_8$ (Kfs)	71.546	84.196	81.632	0.000	0.000	0.000	0.000	0.000	1.216	1.347

4.4 Spinel

The analysed spinel from the Pc3/6 shows a variation in chemical composition (Table 12). Spinel compositions were analysed in different microstructural settings, i.e. as intergrowths in magnetite and inclusions in garnet. Spinel grains included in magnetite exhibit high Al_2O_3 contents (57.57 wt%), low Cr_2O_3 (2.67 wt%), and moderate FeO (29.86 wt%) and MgO (6.41 wt%). These grains are chemically distinct from those associated with garnet rims, which show higher FeO (up to 36.93 wt%), elevated Cr_2O_3 (up to 4.64 wt%), and significantly lower MgO (as low as 2.76 wt%).

The Fe/(Fe + Mg) ratio in spinel varies from 0.71–0.88, with the highest values recorded in garnet rim-associated spinel. The Cr/(Cr + Al) ratio remains low (0.00–0.06), consistent with the composition of aluminous spinel in metapelitic rocks.

Table 12. Representative SEM-EDS mineral analyses of spinel from the sample Pc3/6.

Sample (wt%)	**Pc3/6**								
Analysis number	2.25	8.3	12.1	12.2	**Formula**	2.25	8.3	12.1	12.2
	In magnetite	In Grt core	In Grt rim	In Grt rim		In magnetite	In Grt core	In Grt rim	In Grt rim
SiO_2	0.00	0.44	0.73	0.52	**Si**	0.000	0.100	0.173	0.123
TiO2	0.00	0.00	0.00	0.00	**Ti**	0.000	0.000	0.000	0.000
Al_2O_3	57.57	57.71	50.18	50.64	**Al**	15.289	15.385	14.053	14.096
Cr_2O_3	2.67	0.39	4.64	4.64	**Cr**	0.476	0.070	0.872	0.866
V_2O_3	0.49	0.51	1.31	1.49	**V**	0.089	0.092	0.250	0.282
FeO	29.86	29.59	36.93	35.04	**Fe(ii)**	5.627	5.597	7.338	6.920
MnO	0.00	0.00	0.00	0.000	**Mn**	0.000	0.000	0.000	0.000
MgO	6.41	6.65	2.76	4.30	**Mg**	2.154	2.243	0.978	1.514
CaO	0.00	0.00	0.00	0.00	**Ca**	0.000	0.000	0.000	0.000
ZnO	2.64	3.84	3.28	2.60	**Zn**	0.439	0.641	0.575	0.453
Sum	99.64	99.13	99.83	99.23	**Sum**	24.073	24.127	24.239	24.255
Fe/Fe+Mg						0.72	0.71	0.88	0.82
Cr/Cr+Al						0.03	0.00	0.06	0.06

5. PHASE EQUILIBRIA MODELLING

Results of the previous geothermobarometry investigations are presented in **Table 13**. Obtained pseudosections (MnNCKFMASHT system) for all the samples, also almandine isopleths for the Bl150 and Pc3/6 samples are shown below. Attempts for P-T calculations for rocks from the Lauksargiai-1 drillcore were made by Birmanaite (2023). P-T conditions obtained by GEOTHERMOBAROMETRY programme from the studied rocks and those from nearby boreholes (Lauksargiai-2 and 5, Pociai 3, and Bliudziai 150) have been reported by Skridlaite et al., 2010, 2014.

Table 13. Geothermobarometric estimations in the studied samples.

Sample	Geothermometer	Geobarometer	T, °C	P, kbar	References
Bl150	Grt-Bt, Hodges and Spear, 1982	Grt–Pl–AlSi–Qtz, Koziol and Newton, 1988	700	6	Skridlaite et al., 2014
	Grt-Crd, Lavrent'eva and Perchuk, 1981	Grt-Crd, Aranovich and Podleskiy, 1982	535 – 555	4.1 – 4.3	Skridlaite et al., 2014
P3/6	Grt-Crd, Lavrent'eva and Perchuk, 1981	Grt-Crd, Aranovich and Podleskiy, 1982	621	5	Skridlaite et al., 2014
	Grt-Bt, Hodges and Spear, 1982	Grt–Pl–AlSi–Qtz, Koziol and Newton, 1988	580	5.2	Skridlaite et al., 2014

The bulk rock composition from Western Lithuania received from the XRF spectrometry was normalised and used for modelling of peak and post-peak metamorphism.

Previously, the hp04ver (Holland and Powell, 1998; 2004 upgrade) was used for the sample Lk1D, but it is quite outdated. Phase equilibria modelling was conducted for the sample Lk1D, using Perple_X software (version 7.1.13; Connolly, 1950, 2005) with the hp62 dataset (Holland and Powell, 2011). P-T pseudosection was calculated in the range of 4-9 kbar and 500-1200°C. Isopleths have been calculated with Perple_X for almandine endmember.

The peak mineral assemblage for the **Lk1D** sample is – garnet + melt + k-feldspar + plagioclase + ilmenite + sillimanite + quartz. The obtained model yields the peak metamorphism (P-T) conditions at 5.8-10 kbar and temperature of 810-1130°C. The inferred P-T path is clockwise (Fig. 6). After the peak metamorphism temperature has increased (+ spinel), pressure decreased (+ cordierite). Almandine isopleths from the model match the Lk1D values at lower temperature.

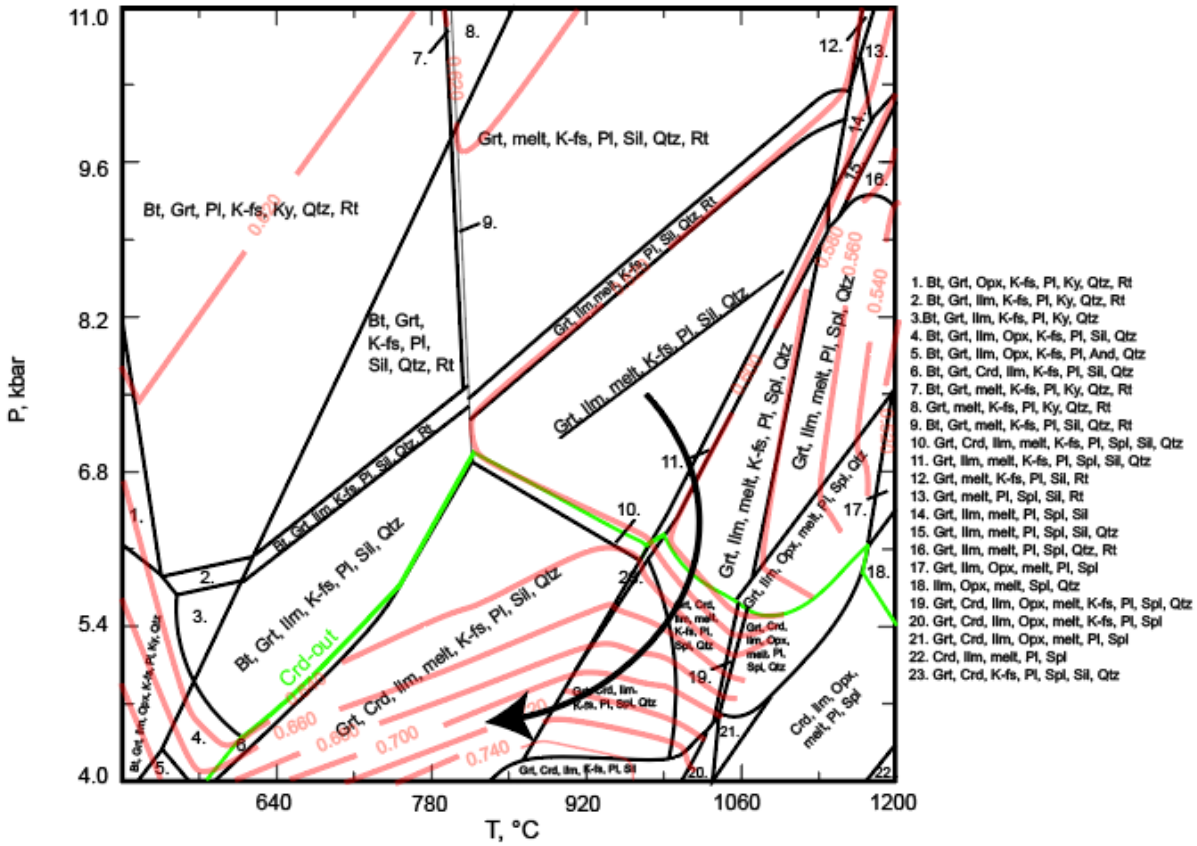

Fig. 6. P-T phase equilibrium diagram (pseudosection) and almandine isopleths (red lines) for the sample Lk1D in the chemical system MnO-Na_2O-CaO-K_2O-FeO-MgO-Al_2O_3-SiO_2-H_2O-TiO_2 (MnNCKFMASHT). Abbreviations: And – andalusite, Bt – biotite, Crd – cordierite, Grt – garnet, Ilm – ilmenite, K-fs – K-feldspar, Ky – kyanite, Opx – orthopyroxene, Pl – plagioclase, Qtz – quartz, Rt – rutile, Sil – sillimanite, Spl – spinel. Black arrow shows a clockwise P-T path. The peak metamorphism mineral assemblage is underlined (Grt + Ilm + melt + K-fs + Pl + Sil +Qtz).

Phase equilibria modelling was conducted for the sample **Bl150**, using the hp62 dataset (Holland and Powell, 2011). P-T equilibrium phase diagram was calculated in the range of 2-8 kbar and 500-900°C.

The resulting pseudosection displays a broad stability field for garnet + biotite + melt + K-feldspar + plagioclase + ilmenite + sillimanite + spinel (field 20), consistent with petrographic observations. The obtained model yields the peak metamorphism (P-T) conditions from 6.2 – 7.2 kbar and temperature of 850 – 880°C. The inferred P-T path is clockwise. After the peak metamorphism temperature has decreased.

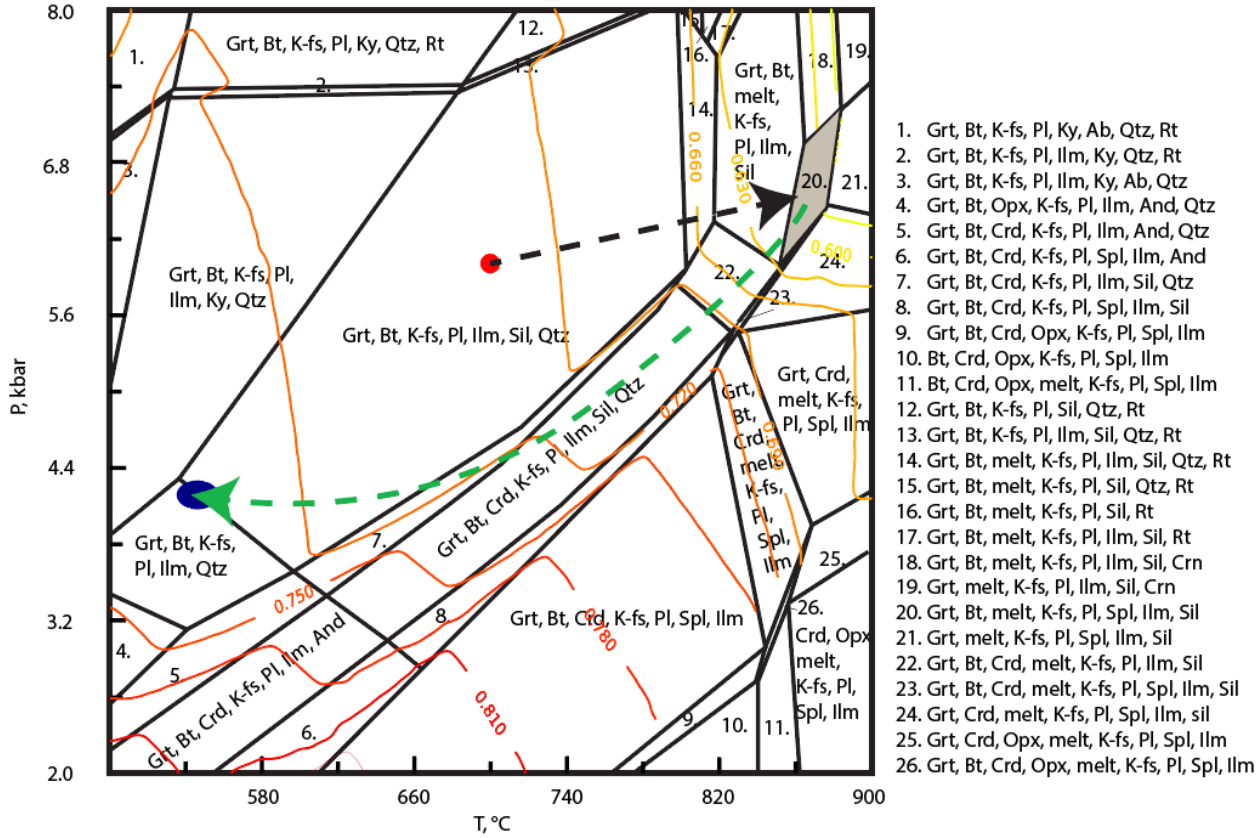

Fig. 7. P-T phase equilibrium diagram (pseudosection) in the chemical system MnO-Na_2O-CaO-K_2O-FeO-MgO-Al_2O_3-SiO_2-H_2O-TiO_2 (MnNCKFMASHT) and almandine isopleths (red to yellow lines) for the Bl150 sample. Abbreviations: And – andalusite, Bt – biotite, Crd – cordierite, Crn – Corundum, Grt – garnet, Ilm – ilmenite, K-fs – potassium feldspar, Ky – kyanite, Opx – orthopyroxene, Pl – plagioclase, Qtz – quartz, Rt – rutile, Sil – sillimanite, Spl – spinel. The stability field for the observed peak metamorphic assemblage (Grt + Bt + melt + K-fs + Pl + Ilm + Sil + Spl) is shaded in grey. Black arrow shows prograde path, green arrow shows retrogression. The results of thermobarometry calculations are shown by red dot – highest temperature (700°C at 6 kbar), and blue eclipse – lowest temperature (535 – 555 °C at 4.1 – 4.3 kbar) from Skridlaite et al., 2014.

Phase equilibria modelling was conducted for the sample **Pc3/6**, using the hp62 dataset (Holland and Powell, 2011). P-T equilibrium phase diagram was calculated in the range of 2-9 kbar and 400 – 800°C (Fig. 8).

The peak mineral assemblage for the Pc3/6 sample is – biotite + garnet + k-feldspar + sillimanite + rutile + quartz. The modelling results compared with the previous thermobarometry results (Fig. 8) record quite complicated history of metamorphism. It includes peak parameters recorded by the mentioned above peak assemblage, the retrogression, followed by the formation of cordierite and a different composition garnet, with subsequent reheating marked by the coexistence of garnet and cordierite. Almandine isopleths from model match the geothermobarometric P-T estimations reported by Skridlaite et al., 2014.

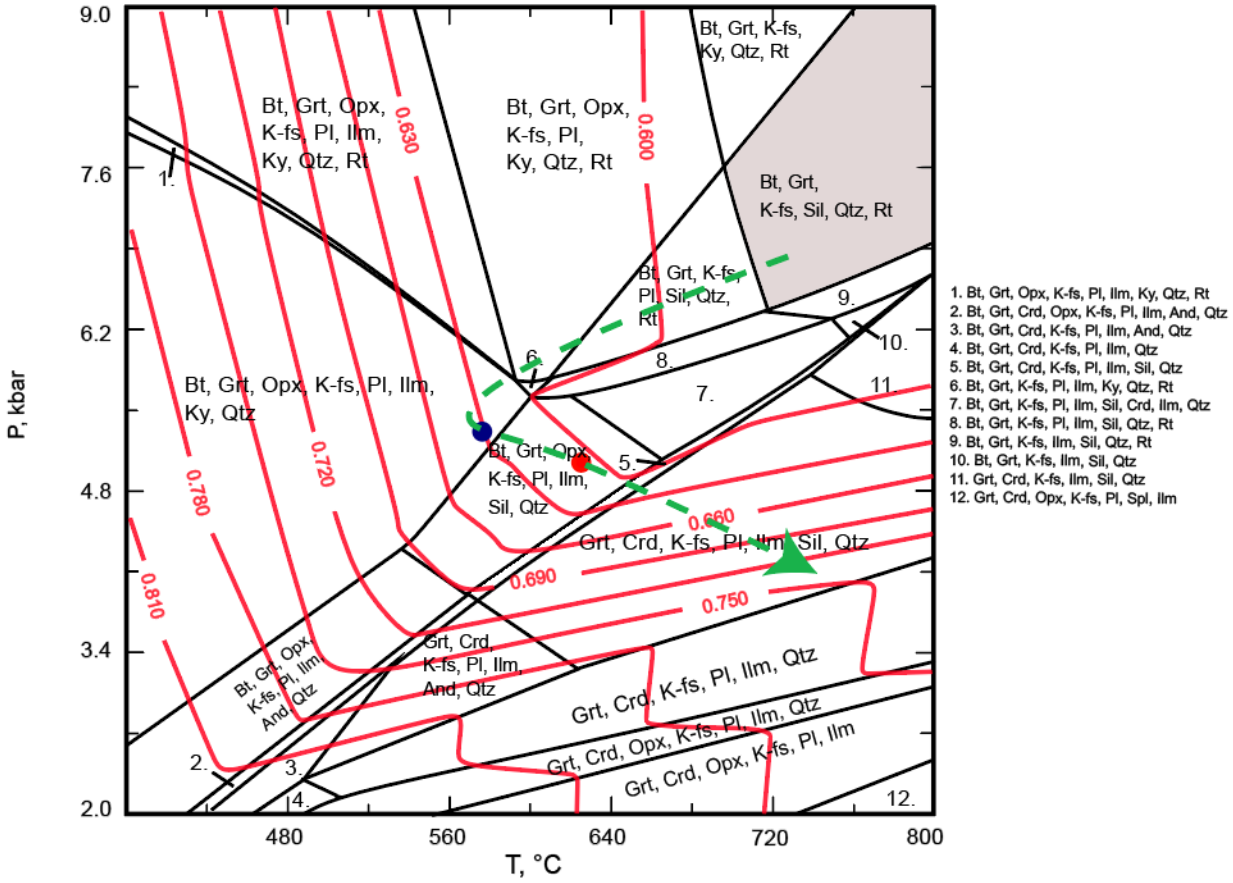

Fig. 8. P-T phase equilibrium diagram (pseudosection) for the sample Pc3/6 in the chemical system MnO-Na_2O-CaO-K_2O-FeO-MgO-Al_2O_3-SiO_2-H_2O-TiO_2 (MnNCKFMASHT) and almandine isopleths (red lines). Abbreviations: And – andalusite, Bt – biotite, Crd – cordierite, Grt – garnet, Ilm – ilmenite, K-fs – K-feldspar, Ky – kyanite, Opx – orthopyroxene, Pl – plagioclase, Qtz – quartz, Rt – rutile, Sil – sillimanite, Spl – spinel. The stability field for the observed peak metamorphic assemblage (Grt + Bt + K-fs + Sil + Qtz + Rt) is shaded in grey. Green arrow shows retrogression and then reheating. The results of thermobarometry calculations are shown by red dot – highest temperature (621°C at 5 kbar), and blue eclipse – lowest temperature (580°C at 5.2 kbar) from Skridlaite et al., 2014.

Phase equilibrium calculations have uncertainties, some of which are quantifiable and some of which are not. In this case, uncertainty ± 1 kbar and P uncertainty ± 50°C are estimated for most P-T constraints derived from pseudosections.

6. GEOCHRONOLOGY

In this study. several samples of the metasedimentary and metaigneous high-grade rocks from the WLG domain described above were chosen to determine the age of their peak conditions and evolution.

The EPMA method allowed dating of monazite grains in areas where metamorphic reactions were recognized (in polished thin sections), thus providing an opportunity to correlate the obtained ages directly with the metamorphic events. The WLG metapelites (samples Lk1/2, Pc3/6, and Bl150) were selected for monazite dating were first checked for their composition, and then the more representative grains were chosen for detailed analysis. The results are in Table 14.

Monazites from sample L1/2 were used for geochronological dating instead of those from **Lk1D** sample, but they both come from the same rock in the same Lauksargiai-1 borehole. For the L1/2, numerous grains of various sizes were identified under the optical microscope (Fig. 9). This sample has a broader range of grain sizes, most fall in the 100-250 μm range. Monazites appear relatively homogeneous and weakly zoned. Most grains are surrounded by garnet, feldspar, quartz, biotite, cordierite.

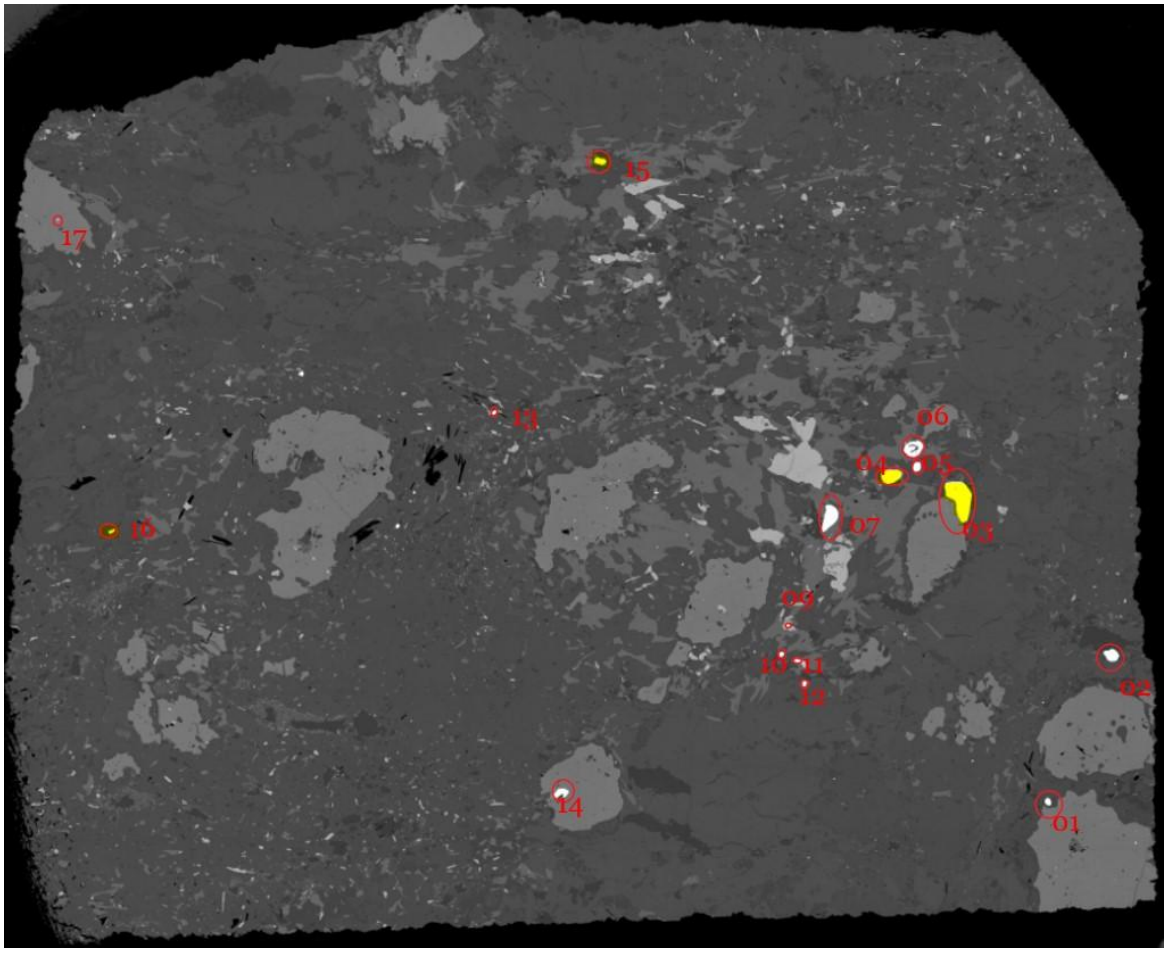

Fig. 9. Photomicrograph (SEM-BSE image) of the L1/2 sample with location of the dated monazite grains (Huć, 2020)

Monazites had at least two distinct age groups: ca. 1.77 Ga and 1.6-1.7 Ga (Huć, 2020).

Monazites are very small in the deformed metapelitic granulite **Pc3/6** (Fig. 10). Back-scattered electron (BSE) imaging showed that, homogeneous and poorly zoned monazites occur in the vicinity of cordierite, garnet and opaque minerals. Monazites with visible zoning occur within cordierite,

garnet and K-feldspars. In the Pc3/6 section, most monazites showed zonation due to the content of Th and Y and no clear zoning was observed due to the content of Pb (Górska, 2020).

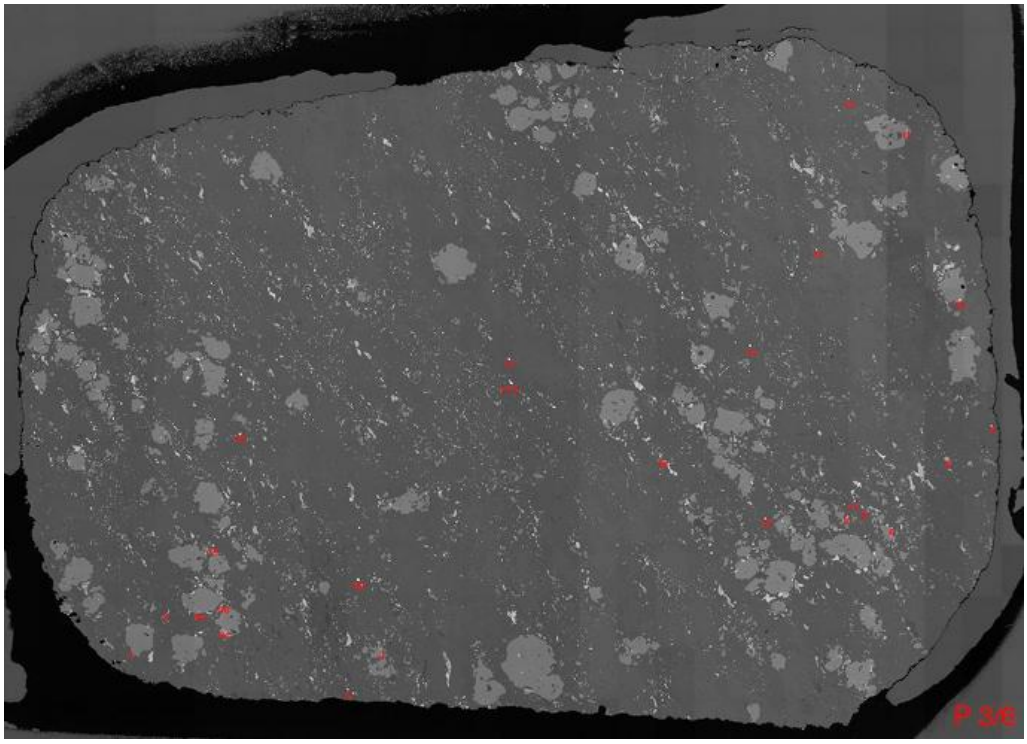

Fig. 10. Photomicrograph (SEM-BSE image) of the Pc3/6 sample with location of the dated monazite grains (Górska, 2020)

It can be assumed that monazites in the examined section show at least two separate episodes of crystallization: ca 1.76 – 1.79 Ga and 1.53-1.57 Ga (Górska, 2020).

The results of earlier dating of monazites from **Bl150** sample were presented in Skridlaite et al. (2014), however some earlier unpublished, newly calculated data is presented here.

Monazite grains located in cordierite preserve cores dated at ca. 1.84 Ga with the highest Y content (Fig. 11) reaching 2.5-3 wt. %. They are usually overgrown by the younger monazite. Such crystals appear in the residual part of the rock (paleo or mesosome).

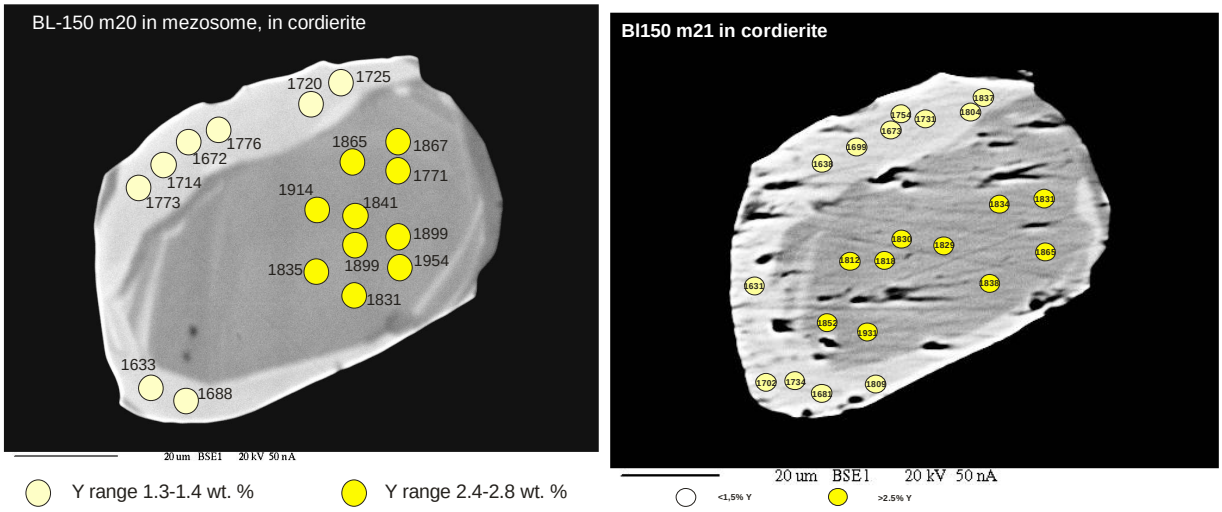

Fig. 11 Monazite grains in cordierite from Bl150 sample (SEM-BSE images) used for geochronological dating by EPMA. Note the older (dark grey) cores overgrown with lighter rims (unpublished data, B. Baginski's personal communication).

The overgrowths record ca. 1.70-1.72 Ga age which is consistent with the 1.71 Ga monazite yielded by several monazite grains and coinciding with the high-grade metamorphic event of 1.73–1.68 Ga in the WLG (Skridlaite et al., 2014). Homogeneous monazite grains from the leucocratic melt parts (perthite) with low Y content (below 0.3 wt.%) as well as higher Th (above 4 wt.%) yielded an age of 1.62-1.63 Ga (1.64 Ga in Skridlaite et al., 2014).

Geochronological dating helped to correct terrain boundaries from north to south in western Lithuania and to define a sequence of crust-forming events (summarized in Table 14).

Table 14. Summary of ages of metamorphic monazite for Proterozoic rocks of Western Lithuania.

Rock/sample	Mineral	Age, Ga	Method	Reference
1.81–1.79 Ga granulite event				
Lk1/2, Lk1D	Monazite	1.77	EPMA	This study
Pc3/6 metapelite	Monazite	1.76 – 1.79	EPMA	This study
1.73–1.68 Ga high grade event				
Bl150 metapelite	Monazite	1.7-1.72	EPMA	Skridlaite et al.. 2014
1.63–1.59 Ga high grade event				
Lk1/2, Lk1D granulite	Monazite	1.6 – 1.7	EPMA	This study
Bl150/1511 metapelite	Monazite	1.62 – 1.63	EPMA	Skridlaite et al.. 2014
1.53–1.50 Ga granulite event				
Pc3/6	Monazite	1.53 – 1.57	EPMA	This study

7. DISCUSSION

The rocks from the Precambrian of Western Lithuania have experienced a multi-stage metamorphism, therefore are difficult to model using thermodynamic programmes. Bulk rock composition showed that the metasedimentary granulites (Lk1D, Pc3/6, and Bl150) are mostly high-alumina, ferruginous pelites. The whole rock bulk composition comprises several compositions of different parageneses, and not always corresponds to the peak ones. A careful study of rock microstructures, mineral chemical compositions, metamorphic reactions combined with results of the thermodynamic modelling, thermobarometry and geochronology data allowed reconstruction of metamorphic types in the studied metapelites from Lk1D, Bl150 and Pc3 samples and imply their tectonic evolution as described below.

The sample Lk1D is an example of both thermal and regional metamorphism. The regional metamorphism may be represented by a peak assemblage of – garnet + melt + k-feldspar + plagioclase + ilmenite + sillimanite + quartz at T exceeding 815^{o}C and P more than 6.8 kbar. The sample contains peritectic garnet which is surrounded by leucocratic domains (melt) and melanocratic part (restite; Fig. 2). Furthermore, the garnet appears to be diffused (almandine isopleths match sample values in lower pressure and temperature; Fig. 6), indicating a second stage of metamorphism. Drop in pressure was followed by the cordierite formation. The cordierite stability field coincides with garnet isopleths (Fig. 6). It seems that the thermal event has affected the rock at 4-5.4 kbar pressure and 1000-1050^{o}C temperature (Fig. 6). The high T, low P metamorphism recorded in this sample likely corresponds with a large igneous event. The neighbouring Transscandinavian Igneous Belt (TIB 2; Skridlaite et al., 2021) in south-central Sweden might be responsible for the associated heat flow in Western Lithuania at 1.60-1.70 Ga as indicated by the monazite ages (Table 14).

The sample Bl150 appears to have been subjected to thermal (contact) metamorphism after the peak metamorphism indicated by the outlined field in Fig. 7 at ca. 1.70 Ga (Table 14). The 1.84 Ga cores preserved in some monazites are relics of an igneous event and match with the rock emplacement age later than 1.85 Ga (Skridlaite et al., 2014). The model shows a clockwise P-T path. Almandine isopleths match the stability field at lower pressures of 4 kbar and temperatures of 700-800^{o} C (Fig. 7). It is possible that the 1.62 – 1.63 Ga metamorphism in the metapelite can be related to an anorogenic granitic magmatism e.g. the Riga intrusion of rapakivi-granitic and anorthositic rocks, that penetrates the northernmost part of the WLG (Kirs et al., 2004; Skridlaite et al., 2014) and to the mafic magmatism in central Sweden (Soderlund et al., 2005). Phase equilibria modelling confirms the high-grade peak assemblage with partial melting conditions.

The Pc3/6 rock has experienced a complicated, multistage metamorphic evolution. The fine-grained garnet, biotite, cordierite, opaque minerals bearing gneiss is strongly deformed (mylonitized; Fig. 4). Quite low metamorphic parameters of 580-620^{o}C and 5 kbar were obtained by garnet, biotite and cordierite geothermobarometers (Table 13). It seems that garnet and biotite compositions were re-equilibrated at lower T and P after the peak (Fig. 8). The peak might be outlined by a matching mineral assemblage field in Fig. 8. Likely, the T exceeded 800^{o}C, while pressure could reach 8 kbar (Fig. 8). Almandine isopleths suggest that the metamorphic conditions are characteristic of contact metamorphism (Fig. 8). It is possible that the rock was retrogressed after the peak, deformed by the ascent of neighbouring intrusions of the Nemunas massif, and subsequently reheated at 1.53-1.57 (Table 14). The phase equilibria model contains orthopyroxene, which is not consistent with petrographic analysis. It is probably because of the lack of plagioclase, or a wrong solid solution model was chosen.

Although isopleths on the calculated P–T pseudosections provide a guide to mineral chemistry, direct comparison with SEM-EDS analyses reveals some mismatches. These arise chiefly because (i) the thermodynamic datasets and activity–composition models assume ideal equilibrium, whereas the rocks examined preserve kinetic disequilibria and retrogressive overprint; (ii) zoned minerals such as biotite and plagioclase display spatially variable compositions, so a point analysis may not reflect the bulk composition assumed by the model; (iii) a single compositional ratio fixed in an isopleth (e.g., X_{Mn}) can be reached via several covariant elemental pathways in natural systems.

Precise P–T conditions cannot be defined because “frozen” mineral reactions, zoned minerals, element diffusion, and scattered monazite U–Th–Pb ages suggest that at least two thermal pulses have affected the area, with monazite-producing reactions and subsequent mineral growth. That is the possible reason, why high-grade events overlap, so it makes difficult to connect rock with a particular event.

CONCLUSIONS

The results of this study provide new insights into rock and mineral chemistry and the metamorphism in the Precambrian rocks of Western Lithuania

The results of the thermodynamic modelling have allowed to constrain P-T parameters, and, combined with the geochronological data, to extend and to refine the stages of tectonic evolution in western Lithuania: The Lk1D rock have been subjected to thermal (contact) (at 1.6 – 1.7 Ga) and regional (at 1.77 Ga) metamorphism. Thermal event was clearly outlined in model.

The Bl150 sample shows thermal metamorphism (at 1.62 – 1.63 Ga). The presumably older field of the peak metamorphism (garnet + biotite + melt + K-feldspar + plagioclase + ilmenite + sillimanite + quartz + spinel) was outlined during the phase equilibria modelling.

The Pc3/6 sample shows a few types of metamorphism: regional (at 1.76 – 1.79 Ga) and deformational followed by reheating (at 1.53-1.57 Ga). The field of the peak metamorphism with the peak assemblage of garnet + biotite + K-feldspar + sillimanite + quartz + rutile was outlined in the P-T space.

ACKNOWLEDGMENTS

I would like to express my deepest gratitude to my academic advisor Assoc. Prof. Gražina Skridlaitė for experience, knowledge, time, and invaluable patience. This study would not be possible without Nature Research Centre in Lithuania, thank you for all the geological material and SEM-EDS analysis. Special thanks to Dr. Laurynas Šiliauskas from Nature Research Centre for helping and answering all questions, Prof. Boguslaw Baginski, Agnieszka Huc, and Klara Gorska from the University of Warsaw for monazite dating and interpretation.

I would like to thank my family, who provided emotional support and encouragement during this stressful time.

The petrographic investigations were carried out using the equipment purchased from funding from the Research Council of Lithuania (LMTLT), agreement No. P-MIP-23-129.

REFERENCES

Aranovich, L. Y., & Podleskii, K. K. (1982). Equilibrium: garnet+ sillimanite+ quartz= cordierite. Thermobarometry of natural assemblages. *Mineralogicheskii Zhurnal*, *2*, 14-20.

Auzanneau, E. et al. (2010) Titanium in phengite: a geobarometer for high temperature eclogites. *Contributions to mineralogy and petrology*. 159 (1). p. 1–24.

Birmanaite, U. (2023) *Peak conditions (P-T) in the Precambrian rocks of Lauksargiai-1 drillcore: mineral composition and phase equilibria modelling*. Bachelor's thesis. Vilnius: Vilnius university.

Bogdanova, S., Bibikova, E., & Gorbatschev, R. (1994) Palaeoproterozoic U-Pb zircon ages from Belorussia: New geodynamic implications for the East European Craton. *Precambrian Research*, *68*(3-4), 231-240. Available at: https://doi.org/10.1016/0301-9268(94)90031-0.

Bogdanova, S., Gorbatschev, R. & Garetsky, R. G. (2016) Europe|east European craton. In: *reference module in earth systems and environmental sciences*. Encyclopedia Geol. 2005, 34–49. Available at: https://doi.org/10.1016/B978-0-12-409548-9.10020-X.

Bogdanova, S., Gorbatschev, R., Skridlaite, G., Soesoo, A., Taran, L. & Kurlovich, D. (2015) Trans-Baltic Palaeoproterozoic correlations towards the reconstruction of supercontinent Columbia/Nuna. *Precambrian Research*, *259*, 5-33. Available at: https://doi.org/10.1016/j.precamres.2014.11.023.

Brown, M. (2002) Retrograde processes in migmatites and granulites revisited. *Journal of Metamorphic Geology*, *20*(1), 25-40. Available at: https://doi.org/10.1046/j.0263-4929.2001.00362.x.

Capitani, C. & Petrakakis, K. (2010) The computation of equilibrium assemblage diagrams with Theriak/Domino software. *American Mineralogist*, *95*(7), 1006-1016. Available at: https://doi.org/10.2138/am.2010.3354.

Coggon, R. & Holland, T. J. B. (2002) Mixing properties of phengitic micas and revised garnet-phengite thermobarometers. *Journal of Metamorphic Geology*, *20*(7), 683-696. Available at: https://doi.org/10.1046/j.1525-1314.2002.00395.x.

Connolly, J. A. D. (1990) Multivariable phase diagrams: An algorithm based on generalized thermodynamics. *American Journal of Science*, *290*, 666–718. Available at: https://doi.org/10.2475/ajs.290.6.666.

Connolly, J. A. D. (2005) Computation of phase equilibria by linear programming: A tool for geodynamic modeling and its application to subduction zone decarbonation. *Earth and Planetary Science Letters*, *236*, 524–541. Available at: https://doi.org/10.1016/j.epsl.2005.04.033.

Gorbatschev, R. & Bogdanova, S. (1993) Frontiers in the Baltic Shield. *Precambrian Research*, *64*(1-4), 3-21. Available at: https://doi.org/10.1016/0301-9268(93)90066-B.

Górska, K. (2020) Chemical dating of monazites: tutorial summary 2019/2020, under supervision of Prof. Bagiński, B., with the help of Dr. Jakubauskas, P. and Kotowski, J., Unpublished.

Hodges, K. V., & Spear, F. S. (1982) Geothermometry, geobarometry and the Al2SiO5 triple point at Mt. Moosilauke, New Hampshire. *American mineralogist*, *67*(11-12), 1118-1134.

Holdaway. M. (2000) Application of new experimental and garnet Margules data to the garnet-biotite geothermometer. American Mineralogist. Vol. 85 (Issue 7-8). p. 881-892. doi: 10.2138/am-2000-0701

Holland, T. & Powell, R. (1996) Thermodynamics of order-disorder in minerals: II. Symmetric formalism applied to solid solutions. *American Mineralogist*, *81*(11-12), 1425-1437. Available at: https://doi.org/10.2138/am-1996-11-1215.

Holland, T. & Powell, R. (2001) Calculation of phase relations involving haplogranitic melts using an internally consistent thermodynamic dataset. *Journal of Petrology*, *42*(4), 673-683. Available at: https://doi.org/10.1093/petrology/42.4.673.

Holland, T. J. B. & Powell, R. (1998) An internally consistent thermodynamic data set for phases of petrological interest. *Journal of Metamorphic Geology*, *16*(3), 309-343. Available at:

https://doi.org/10.1111/j.1525-1314.1998.00140.x.

Holland, T. J. B. & Powell, R. (2011) An improved and extended internally consistent thermodynamic dataset for phases of petrological interest, involving a new equation of state for solids. *Journal of Metamorphic Geology*, *29*(3), 333-383. Available at: https://doi.org/10.1111/j.1525-1314.2010.00923.x.

Huć, A. (2020) Datowanie chemiczne monacytów: podsumowanie tutorialu 2019/2020, pod opieką prof. Bagińskiego, B., z podziękowaniami dla dr. Jakubauskasa, P. i mgr. Kotowskiego, J., Unpublished.

Jennings, E. S., & Holland, T. J. (2015) A simple thermodynamic model for melting of peridotite in the system NCFMASOCr. *Journal of Petrology*, *56*(5), 869-892.

Kirs, J., Haapala, I., & Rämö, O. T. (2004) Anorogenic magmatic rocks in the Estonian crystalline basement. In *Proceedings of the Estonian Academy of Sciences. Geology* (Vol. 53, No. 3, pp. 210-225).

Koziol, A. M., & Newton, R. C. (1988) Redetermination of the anorthite breakdown reaction and improvement of the plagioclase-garnet-Al2SiO5-quartz geobarometer. *American Mineralogist*, *73*(3-4), 216-223.

Lanari, P. and Duesterhoeft, E. (2019) Modelling metamorphic rocks using equilibrium thermodynamics and internally consistent databases: Past achievements, problems and perspectives. Journal of Petrology, 60(1), pp.19-56. Available at: https://doi.org/10.1093/petrology/egy105

Lavrent'eva, I. V., & Perchuk, L. L. (1981) Cordierite–garnet thermometer. In *Dokl. Akad. Nauk SSSR* (Vol. 259, No. 3, pp. 697-700).

Newton, R. C., Charlu, T. V., and Kleppa, O. J. (1980) Thermochemistry of the high structural state plagioclases. Geochimica et Cosmochimica Acta, 44(7), 933-941. Available at: https://doi.org/10.1016/0016-7037(80)90283-5

Powell, R. and Holland, T. (2010) Using equilibrium thermodynamics to understand metamorphism and metamorphic rocks. Elements 6, pp.309–314. Available at: https://doi.org/10.2113/gselements.6.5.309

Putnaite J., Skridlaite G. (2021) P-T evolution of the Proterozoic aluminous granulites from the western East European Craton, West Lithuania. Metamorphic Studies Group 40th anniversary Research in Progress meeting 2021, online, 29–31 March 2021.

Reed, S.J.B. (2005) Electron microprobe analysis and scanning electron microscopy in geology. Cambridge university press, pp. 159, 160.

Siliauskas, L., Skridlaite, G., Baginski, B., Whitehouse, M., & Prusinskiene, S. (2018) What the ca. 1.83 Ga gedrite-cordierite schists in the crystalline basement of Lithuania tell us about the late Palaeoproterozoic accretion of the East European Craton. *GFF*, *140*(4), 332-344.

Skridlaite, G. and Motuza, G. (2001) Precambrian domains in Lithuania: evidence of terrane tectonics. *Tectonophysics*. 339 (1–2). 113–133. Available at: https://doi.org/10.1016/S0040-1951(01)00035-X

Skridlaite, G. et al. (2014) Recurrent high grade metamorphism recording a 300Ma long Proterozoic crustal evolution in the western part of the East European Craton. *Gondwana research*. [Online] 25 (2). 649–667.

Skridlaite, G. et al. (2021) On the origin and evolution of the 1.86–1.76 Ga Mid-Baltic Belt in the western East European Craton. *Precambrian research*. [Online] 367106403-.

Skridlaite, G., Baginski. B., Bogdanova, S., and Whitehouse, M. (2010. May). Metamorphism and magmatism in the western East European Craton: implications for 1.84 to 1.45 Ga evolution in Lithuania. In *Geophysical Research Abstract* (Vol. 12).

Skridlaite, G., Wiszniewska, J., and Whitehouse, M. (2012) Remnants of the c. 1.83 Ga volcanic island arc in Lithuania: implications for the development of the western East European Craton. *Abstracts. 34th IGC. Brisbaine. Australia*.

Söderlund, U., Isachsen, C.E., Bylund, G. *et al.* (2005) U–Pb baddeleyite ages and Hf, Nd isotope chemistry constraining repeated mafic magmatism in the Fennoscandian Shield from 1.6 to 0.9 Ga. *Contrib*

Mineral Petrol 150, 174–194. Available at: https://doi.org/10.1007/s00410-005-0011-1

Tajčmanová, L, et al. (2009) A thermodynamic model for titanium and ferric iron solution in biotite. *Journal of metamorphic geology*. 27 (2). 153–165.

Vėjelytė, I. (2011) The Telšiai and Drūkšiai-Polotsk Deformation Zones: petrography and U/Pb geochronology.

White, R. W. et al. (2000) The effect of TiO2 and Fe2O3 on metapelitic assemblages at greenschist and amphibolite facies conditions: mineral equilibria calculations in the system K2O-FeO-MgO-Al2O3-SiO2-H2O-TiO2-Fe2O3. Journal of Metamorphic Geology 18:497-511.

White, R. W. et al. (2001) Calculation of partial melting equilibria in the system Na2O-CaO-K2O-FeO-MgO-Al2O3-SiO2-H2O (NCKFMASH). Journal of metamorphic geology. 19 (2). pp. 139–153

Zhao, K. et al. (2017) Crystallization conditions of peraluminous charnockites: constraints from mineral thermometry and thermodynamic modelling. *Contributions to mineralogy and petrology*. 172 (5). 1–19.

SUMMARY

VILNIUS UNIVERSITY
FACULTY OF CHEMISTRY AND GEOSCIENCES

UGNĖ BIRMANAITĖ

Relationship between metamorphism and tectonic settings in the Precambrian rocks of Western Lithuania

The Western Lithuanian Granulite Domain (WLG) is a crystalline basement structure occupying a large part of western Lithuania. The domain is composed of metamorphosed rocks. Felsic and intermediate metaigneous and metasedimentary rocks predominate. Granulites and other high-temperature rocks are important for the identification of geodynamic processes and are also useful for tectonic reconstructions. This work aims to investigate the metamorphism in Western Lithuania (Lauksargiai-1, Bliudžiai-150, and Pociai-3 drillings), to review a new material, to analyse the samples for bulk rock composition, to identify minerals, to (re)constrain peak metamorphism (P-T) parameters using phase equilibria modelling with "Perple_X", to determine age of the peak conditions, and identify the type of metamorphism.

Bulk rock analyses reveal that the investigated metasedimentary granulites (samples Lk1D, Pc3/6, and Bl150) are predominantly high-alumina, ferruginous pelites.

Sample Lk1D records the evidence of both regional metamorphism at ~1.77 Ga and a subsequent thermal (contact) overprint at 1.60–1.70 Ga, the latter of which is clearly supported by phase equilibria modelling.

Sample Bl150 has experienced a peak metamorphism followed by high-temperature thermal metamorphism at 1.62–1.63 Ga. Petrographic analysis and phase equilibria modelling defined the peak metamorphic assemblage: garnet, biotite, melt, K-feldspar, plagioclase, ilmenite, sillimanite, spinel, and quartz, indicating conditions consistent with partial melting.

Sample Pc3/6 reveals a more complex metamorphic history, having undergone regional high-grade metamorphism at 1.76–1.79 Ga, followed by deformation and reheating between 1.53 and 1.57 Ga. During petrographic analysis and phase equilibria modelling the peak assemblage was revealed: garnet, biotite, K-feldspar, sillimanite, quartz, and rutile.

To sum up, the studied samples illustrate the multi-stage metamorphic evolution of the Lithuanian crystalline basement, marked by a dominant regional high-grade metamorphism during the orogeny, followed by more localized high-temperature events during the Mesoproterozoic, driven by the intrusions.

SANTRAUKA

VILNIAUS UNIVERSITETAS
CHEMIJOS IR GEOMOKSLŲ FAKULTETAS

UGNĖ BIRMANAITĖ

Metamorfizmo tipo ryšys su tektonine aplinka prekambro uolienose vakarų Lietuvoje

Vakarų Lietuvos granulitų domenas (VLG) – Lietuvos kristalinio pamato darinys, užimantis didžiąją vakarų Lietuvos dalį. Domene vyrauja metamorfizuotos uolienos. Vakarų Lietuvos granulitų domene pasitaiko felzinės bei vidutinės metamagminės ir metanuosėdinės uolienos. VLG yra plačiai paplitę granulitai, Pocių paleobaseine jie užima didžiulę ploto dalį. Granulitai ir kitos aukštos temperatūros uolienos yra svarbios, norint nustatyti geodinaminius procesus, taip pat naudingos tektoninėms rekonstrukcijoms. Buvo siekiama ištirti prekambro uolienų metamorfizmą Vakarų Lietuvoje (Lauksargiai-1, Pociai-3 bei Bliūdžiai-150 gręžiniuose), peržiūrint naują medžiagą, (iš naujo) įvertinant aukščiausius metamorfizmo salygų (P-T) parametrus, taikant fazių pusiausvyros modeliavimą naudojant „Perple_X" programinę įrangą, nustatant aukščiausių parametrų uolienų amžių bei indentifikuojant metamorfizmo tipą.

Šio tyrimo rezultatai suteikia naujos informacijos apie uolienų ir mineralų cheminę sudėtį bei metamorfizmo raidą vakarų Lietuvos prekambrinėse uolienose. Mėginių (Lk1D, Pc3/6 ir Bl150) cheminės analizės tyrimo rezultatai rodo, kad šie metasedimentiniai granulitai daugiausia yra aliuminingi, geležingi pelitai.

Lk1D mėginyje fiksuojami dviejų tipų metamorfizmo įvykiai: regioninis metamorfizmas prieš maždaug 1,77 mlrd. metų bei vėlesnis terminis (kontaktinis) metamorfizmas prieš 1,60–1,70 mlrd. metų, aiškiai išryškėjęs fazių pusiausvyros modeliavimo metu.

Bl150 mėginyje nustatytas vidutinių parametrų regioninis metamorfizmas, lydimas aukštos temperatūros terminio metamorfizmo, įvykusio prieš 1,62–1,63 mlrd. metų. Gauta maksimalių parametrų mineralų paragenezė yra granatas, biotitas, lydalas, kalio feldšpatas, plagioklazas, ilmenitas, silimanitas, špinelė ir kvarcas.

Pc3/6 mėginys rodo sudėtingesnę metamorfinę raidą: uoliena pirmiausia patyrė regioninį metamorfizmą prieš 1,76–1,79 mlrd. metų, o vėliau buvo deformuota ir pašildyta prieš 1,53–1,57 mlrd. metų. Susiejus petrografinę analizę ir modeliavimo rezultatus gauta maksimalių parametrų mineralų paragenezė: granatas, biotitas, kalio feldšpatas, silimanitas, kvarcas ir rutilas.

Uolienos atspindi daugiaetapę Vakarų Lietuvos kristalinio pamato metamorfinę raidą, kuriai būdingas vyraujantis regioninis aukštos temperatūros metamorfizmas orogenezės metu, po kurio sekė lokalūs aukštos temperatūros įvykiai Mezoproterozojuje, sukelti intruzijų.